

RESEARCH ARTICLE

# Interplay of tectonism and eustasy during the Early Permian icehouse: Southern Sydney Basin, southeast Australia

Angelos G. Maravelis<sup>1</sup>  | Octavian Catuneanu<sup>2</sup> | Adam Nordsvan<sup>3</sup> | Bill Landenberger<sup>4</sup> | Avraam Zelilidis<sup>1</sup>

<sup>1</sup>Laboratory of Sedimentology, Department of Geology, University of Patras, Patras, Greece

<sup>2</sup>Department of Earth and Atmospheric Sciences, University of Alberta, Edmonton, Alberta, Canada

<sup>3</sup>Department of Applied Geology, Curtin University Bentley, Perth, Western Australia, Australia

<sup>4</sup>School of Environmental and Life Sciences, University of Newcastle, Callaghan, New South Wales, Australia

**Correspondence**

Angelos G. Maravelis, Laboratory of Sedimentology, Department of Geology, University of Patras, 26504 Rio, Patras, Greece.  
Email: amaravel@geology.upatras.gr

**Funding information**

NSW Institute for Frontiers Geosciences (IFG)

Handling editor: S. Tyrrell

This investigation presents an outcrop-based integrated study of sedimentological analysis and sequence stratigraphy applied to the Lower Permian sedimentary succession in the southern Sydney Basin, Australia. This succession accumulated in several depositional environments and sub-environments that range from non-marine (fluvial) to marine (outer shelf), representing the fill of a sedimentary basin that resembles a fault-bounded, rift basin. The stratigraphic analysis indicates a deepening-upward trend, and the sequence stratigraphic approach has established that these sediments can be attributed to the lowstand, transgressive, and highstand systems tracts. Lowstand sediments can be defined by fluvial facies that are located between the subaerial unconformity and the maximum regressive surface. Transgressive facies correspond to estuarine, upper and lower shoreface, and inner and outer shelf depositional environments and are located between the maximum regressive and the maximum flooding surfaces. Highstand bottomset sediments are accumulated above the maximum flooding surface and are represented by outer shelf facies. The stratigraphic architecture indicates the development of an almost complete depositional sequence, mainly developed under the control of tectonically induced subsidence, but also influenced by the high sedimentation rates and the high gradient of the inherited topography. Eustatic sea-level fluctuations were of minor importance during the deposition of the examined sediments.

**KEYWORDS**

glacio-eustasy, icehouse periods, Permian, sequence stratigraphy, southern Sydney Basin, tectonics

## 1 | INTRODUCTION

Allogenic factors, which are external to the depositional systems, such as eustasy, tectonics, and climate, play a major role in relative sea-level changes, sediment supply, and environmental energy (Einsele, Ricken, & Seilacher, 1991). Autogenic factors, which are internal to the depositional system and are unrelated to relative sea-level changes and climate (Einsele et al., 1991), may also play a significant role in the stratigraphic architecture (Catuneanu & Zecchin, 2013). The interaction of allocyclic and some autocyclic processes (e.g., avulsion, autoretrete, and delta lobe switching) controls the formation of several sequence stratigraphic surfaces (Castelltort et al., 2003; Catuneanu & Zecchin, 2013; Einsele et al., 1991; Feldman, Franseen, Joeckel, & Heckel, 2005). These processes influence changes in shoreline trajectory, which in turn affect the development of systems tracts in the sedimentary basins (Catuneanu, 2002, 2006). Shallow-marine environments are particularly sensitive to changes in accommodation,

and therefore, they provide a good record of relative sea-level oscillations (Cantalamessa & Di Celma, 2004).

Sequence stratigraphy has been employed as a methodology for enhancing facies predictability and palaeogeographic reconstructions in sedimentary basins (Catuneanu, 2003, 2006; De Gasperi & Catuneanu, 2014; Di Celma, Cantalamessa, Landini, & Ragaini, 2010; Maravelis & Zelilidis, 2011, 2012; Zecchin, Civile, Caffau, Sturiale, & Roda, 2011). Outcrop data offer insights into the physical attributes of stratigraphic surfaces and sediment packages and are important for the high-resolution sequence stratigraphic analysis (Zecchin & Catuneanu, 2013, 2015). The term "sequence" has been recently redefined as "a cycle of change in stratal stacking patterns, defined by the recurrence of the same types of sequence stratigraphic surface through geologic time" (Catuneanu & Zecchin, 2013; Catuneanu et al., 2011). There is a general consensus that sequences may consist of different combinations of systems tracts that are separated by surfaces of sequence stratigraphic significance, which can be observed at different

scales (Catuneanu, 2006; Csato & Catuneanu, 2012, 2014; Csato, Catuneanu, & Granjeon, 2014; Zecchin & Catuneanu, 2013). Sequence stratigraphy has been applied in different tectonic regimes and has unraveled differences in stratigraphic architectures between extensional and compressional settings (Cantalamessa & Di Celma, 2004; Catuneanu, 2004, 2006; Maravelis, Boutelier, Catuneanu, Seymour, & Zelilidis, 2016; Maravelis, Pantopoulos, Tserolas, & Zelilidis, 2017; Martins-Neto & Catuneanu, 2010), as well as between sub-basins of the same sedimentary basin (Catuneanu, Hancox, Cairncross, & Rubidge, 2002; Catuneanu, Sweet, & Miall, 1999; Miall, Catuneanu, Vakarelou, & Post, 2008). The applications of sequence stratigraphy have also been expanded to all depositional settings and from underfilled to overfilled basins of Precambrian to Phanerozoic age (Catuneanu, Khalifa, & Wan, 2006; Catuneanu, Martins-Neto, & Eriksson, 2005; Eriksson, Mazumder, Catuneanu, Bumby, & Ilondo, 2006; Fanti & Catuneanu, 2010).

Icehouse periods are typified by high-frequency sequences whose architecture differs from that of sequences accumulated during greenhouse times (Di Celma & Cantalamessa, 2007; Fielding, Bann, Maceachern, Tye, & Jones, 2006; Isbell, Cole, & Catuneanu, 2008; Zecchin, Caffau, Civile, & Roda, 2010; Zecchin, Catuneanu, & Rebescu, 2015). Transgressive sediments that correspond to the T-cycles of Zecchin (2007) dominate during icehouse periods, whereas greenhouse periods are characterized by regression-dominated sequences (R-cycles

of Zecchin, 2007). T-cycles are metres to a few tens of metres thick, are composed of an incomplete succession of systems tracts, and are top-truncated and vertically stacked (Di Celma & Cantalamessa, 2007; Kidwell, 1997). Several combinations of factors have been invoked to account for the formation of the T-cycles including high-amplitude glacio-eustatic changes (Fielding et al., 2006), relatively high sediment input during transgression with slow relative sea-level rise, when accommodation still exceeds sediment supply (Cantalamessa & Di Celma, 2004) and situations of rapid accommodation creation associated with high sediment supply (Zecchin, 2005, 2007).

The southern Sydney Basin (SSB) offers an opportunity to evaluate some of the above-mentioned attributes. This research documents a Lower Permian sedimentary succession in the south coast region (southeastern Australia; Figure 1). This succession is approximately 700 m thick and is composed of the Wasp Head (WHF, early to mid-Sakmarian, ~100 m), Pebbley Beach (PBF, Sakmarian to Artinskian, ~150 m), and Snapper Point (SPF, early Kungurian, ~300–400 m) formations, as well as the Wandrawandian Siltstone (WS, mid-Kungurian, ~100 m). The studied succession corresponds to a nearly complete depositional sequence. The systems tracts and the nature of stratal surfaces are controlled by both the basin subsidence history and the glacio-eustatic changes during the Permian. This case study brings new field evidence and insights into understanding the sequence stratigraphic architecture that may form during icehouse periods.

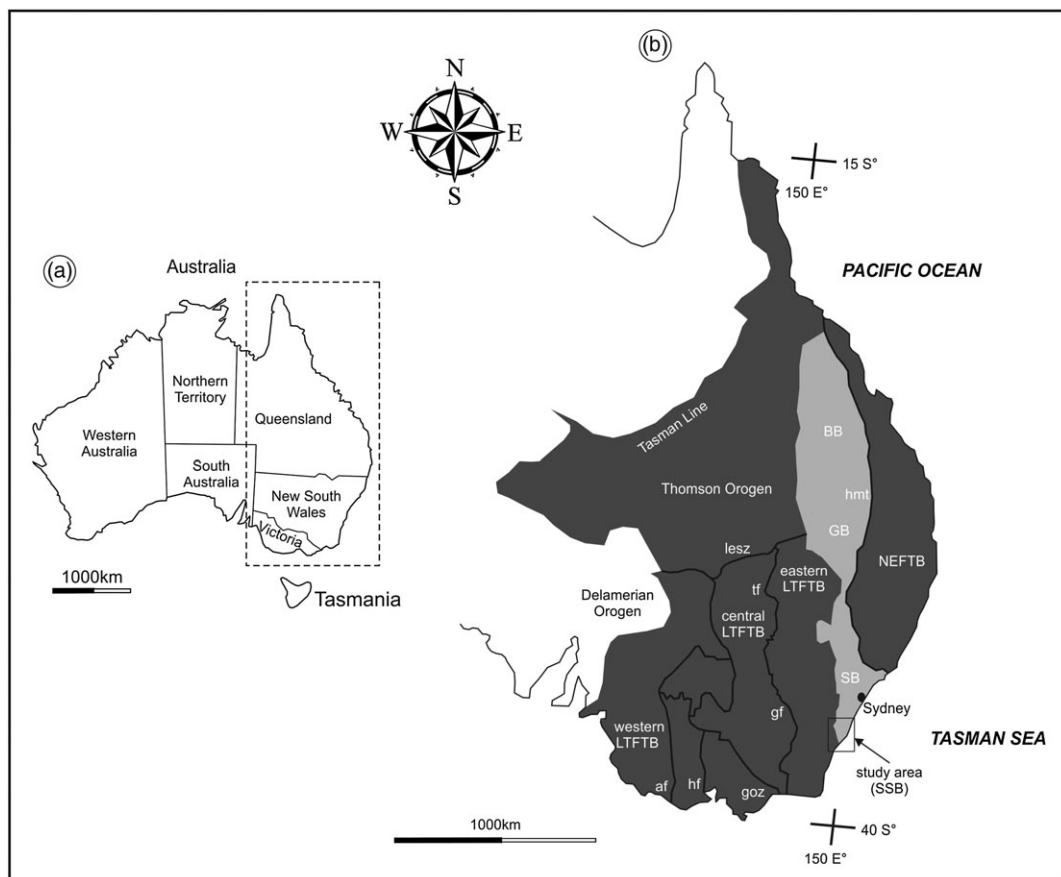


**FIGURE 1** Geological map of Tasmanides in eastern Australia depicting the position of the SSB. af = Avoca Fault; BB = Bowen Basin; GB = Gunnedah Basin; gf = Gilmore Fault Zone; goz = Governor Fault; hf = Heathcote Fault Zone; hmt = Hunter-Mooki Thrust; lesz = Louth-Eumarra Shear Zone; LTFTB = Lachlan-Tasman Fold and Thrust Belt; NEFTB = New England Fold and Thrust Belt; SB = Sydney Basin; SSB = southern Sydney Basin; tf = Tullamore Fault Zone (from Glen, 2013)

## 2 | TECTONO-STRATIGRAPHIC SETTING

The Sydney Basin comprises a complex system of depocentres forming the southern part of the composite Bowen–Gunnedah–Sydney Basin system. It is bounded by the Lachlan–Tasman Fold and Thrust Belt to the southwest (SW) and by the New England Fold and Thrust Belt to the northeast (NE; Veevers, Conaghan, & Powell, 1994). The Bowen–Gunnedah–Sydney Basin corresponds to an important component of the eastern Australian Tasmanides (Figure 1). The Lachlan–Tasman Fold and Thrust Belt is thought to be the principal contributor of sediment into the SSB (Veevers et al., 1994), and it is composed of submarine fans that correspond to the central part of the composite Palaeozoic Tasman Orogen along the eastern margin of Australia (Coney, Edwards, Hine, Morrison, & Windrum, 1990; Scheibner, 1987).

The tectonic evolution of the Lachlan–Tasman Fold and Thrust Belt displays a complex pattern that involves accretion of structurally thickened submarine fans, accretionary prisms, volcanic arcs, and continental and oceanic crust. The resulting crustal thickening occurred during plate convergence in an oceanic setting along the eastern margin of Gondwana (Foster, Gray, & Bucher, 1999; Gray, Foster, & Bierlein, 2002). Oceanic subduction has been invoked to account for the tectonic evolution of the western and central Lachlan–Tasman

Fold and Thrust Belt for parts of their history (Offler, McKnight, & Morand, 1998; Offler, Miller, Grayd, Foster, & Bale, 1998; Spaggiari, Gray, & Foster, 2003). Extension and pronounced magmatism characterize the final stages of the evolution of the belt indicating an Andean- or Cordilleran-type continental margin with effects observed mostly in the central and eastern parts of the Lachlan–Tasman Fold and Thrust Belt (Collins, 2002a; Collins, 2002b; Collins & Hobbs, 2001).

Rifting of the eroded Lachlan–Tasman Fold and Thrust Belt took place during the Early Permian and was responsible for the initial development of the Sydney Basin (Veevers et al., 2006), which displays an evolution from rifts and/or transtensional basins into a foreland basin attached to the New England Fold and Thrust Belt. The stratigraphic evolution of the SSB is depicted on Figure 2. Initial crustal extension is recorded by the accumulation of the shallow-marine WHF and the mostly terrestrial correlative Clyde Coal Measures (Tye, Fielding, & Jones, 1996). The overlying PBF and SPF represent a variety of marine, terrestrial, and basin margin facies that formed during a phase of more uniform, regional subsidence (Fielding et al., 2006). The appearance of tephra in the overlying WS testifies the onset of mid-Permian subduction-related calc-alkaline volcanism along the New England Fold and Thrust Belt (Herbert & Helby, 1980). WS has been interpreted as deposits that have been accumulated in a shelf

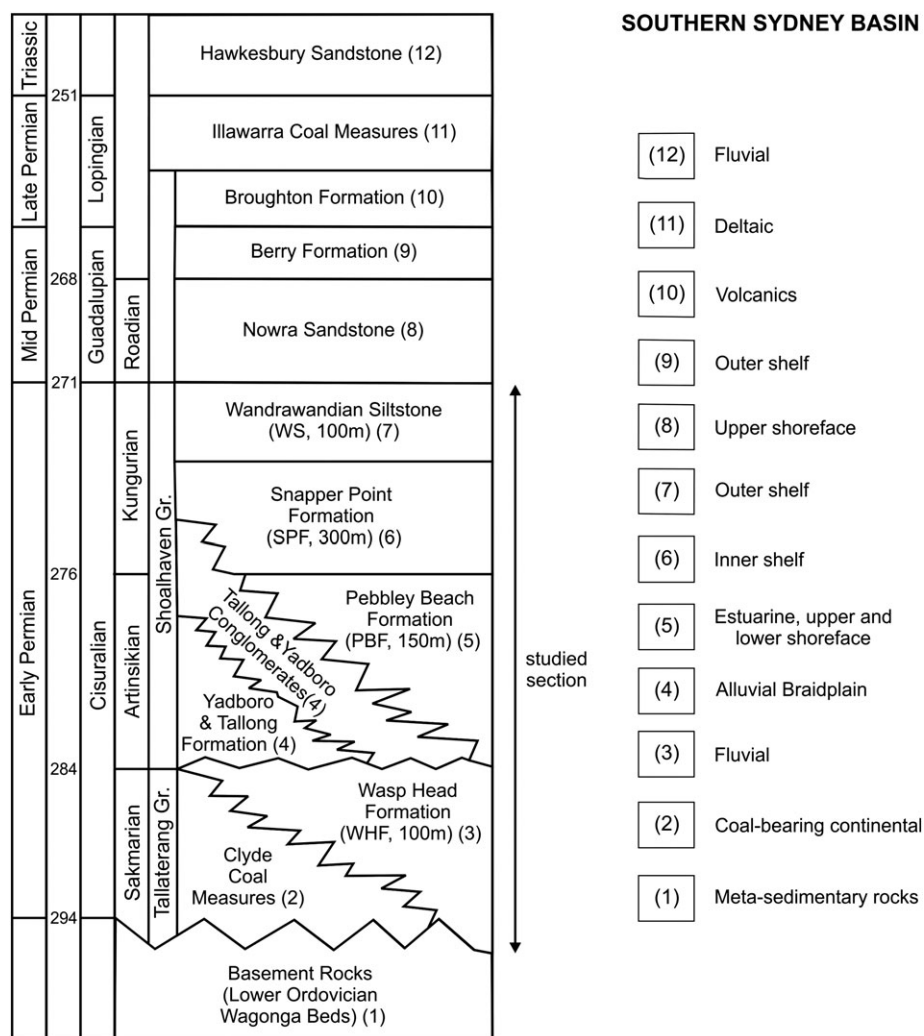


FIGURE 2 Revised lithostratigraphy of the southern Sydney Basin (modified from Tye et al., 1996)

to offshore depositional environment (Thomas, Fielding, & Frank, 2007). The overlying Nowra Sandstone is interpreted as shoreface facies, and the following Berry Siltstone reflects basin-scale transgression and accumulation in an outer shelf depositional environment (Eyles, Eyles, & Gostin, 1998).

The SSB experienced subsequent conversion to a fold-thrust belt by progressive westward thrusting and folding (Veevers et al., 2006). Initiation of the foreland basin system is still controversial and has been placed in the (a) latest Carboniferous (Evans & Migliucci, 1991), (b) end Carboniferous (Scheibner & Veevers, 2000), (c) late Early Permian (Glen & Beckett, 1997), and (d) Late Permian (Retallack, 1999). The evolution of the SSB into a foreland basin and the transition to principally terrestrial sediment accumulation most likely occurred

during the Late Permian time (Fielding et al., 2006). This is marked by the deposition of the Gerringong Volcanics (Broughton Formation) and the Illawarra Coal Measures.

### 3 | METHODS

Twenty-five outcrops from natural cliffs were studied along 40 km of the New South Wales coastline between Ulladulla in the north and Myrtle Beach in the south (Figure 3). Early Permian strata onlap the eastern edge of the Lachlan-Tasman Fold and Thrust Belt, and the complete stratigraphic succession, from WHF to Nowra Sandstone, is outcropped in the coastal headlands. Depositional processes,

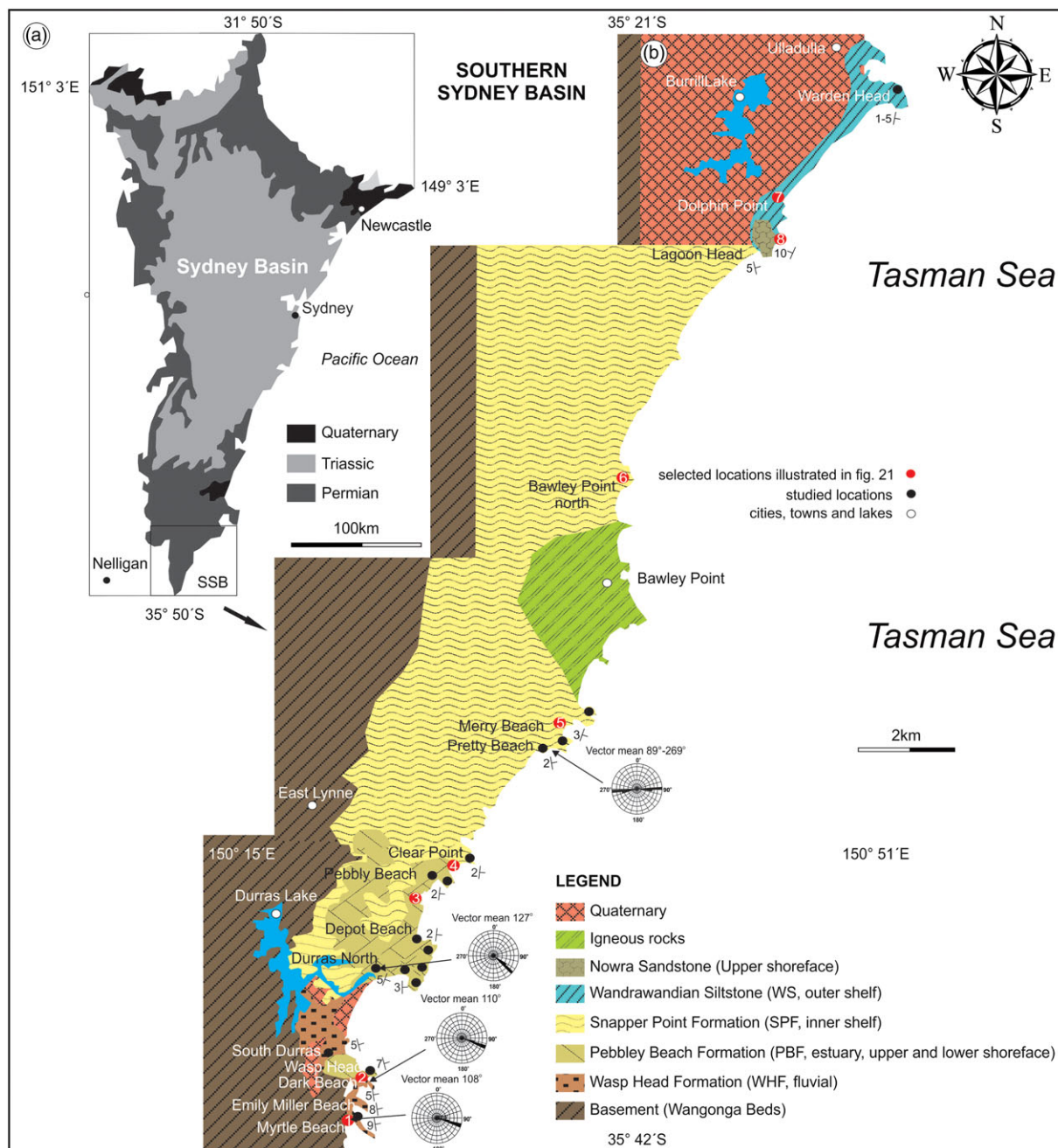


**FIGURE 3** Detailed geological map of the southern Sydney Basin (SSB) depicting the up-sequence evolution during the Early to mid-Permian (modified from Tye et al., 1996; Eyles et al., 1998; Fielding et al., 2006). Black dots correspond to the studied sections. Palaeodispersal analysis is from Fielding et al. (2006) and Rygel et al. (2008a) [Colour figure can be viewed at [wileyonlinelibrary.com](http://wileyonlinelibrary.com)]

**TABLE 1** Summarizing table of facies and facies associations and their main characteristics, in relation to sedimentary structures, depositional environments, and appearance in the southern Sydney Basin

Facies	Description	Sedimentary structures	Facies interpretation	Appearance
F1: clast- to matrix-supported breccia and conglomerate	Thick beds with an often tabular geometry or erosional base; mainly poorly sorted and with sub-angular to sub-rounded clasts (granules to boulders)	Structureless and in places reverse to normal grading. Bullet-shaped clasts are also present.	Bedload transport during high flow regime. Clast supported nature indicates action by braided streams (Nemec & Steel, 1984). The relatively high degree of clast angularity suggests short transport distance (Nichols, 2009), and clast imbrication points at tractional deposition (Whiting et al., 1988).	FA1, FA2, FA4, and FA5
F2: structureless sandstone	Amalgamated sandstone beds with poor sorting and fine to coarse grain size; beds are often tabular, with either sharp or erosional boundaries. Often, parallel-stratified floating large clasts occur.	Unstratified and often mud drapes	Rapid deposition of high-density flows indicating high sedimentation rates that prevent efficient sorting (Lowe, 1988; Magalhães et al., 2015). The occurrence of mud drapes is indicative of tidal influence during the deposition (Reineck & Wunderlich, 1968).	FA1, FA2, FA3, and FA5
F3: trough cross-stratified sandstone	Fine- to very coarse-grained, occasionally pebbly trough cross-bedded sandstone. Such beds are moderately to well-sorted and contain both single sets and co-sets separated by bounding surfaces.	Trough cross-stratification and in places mud drapes	Migration of S-shaped 3D dunes in lower flow regime conditions (Collinson, 1996). The occurrence of mud drapes suggests a tide-influenced depositional environment (Reineck & Wunderlich, 1968).	FA1, FA2, FA3, FA4, and FA5
F4: sigmoidal cross-stratified sandstone	Fine- to medium-grained sandstone	Cross-stratification with sigmoidal profile and often mud drapes	They form when bedforms with a concave lee slope climb at relatively high angles such that the erosional bounding surface passes close to the bedform crest (Allen, 1982). The occurrence of mud drapes is indicative of tidal influence during the deposition (Reineck & Wunderlich, 1968).	FA4
F5: planar cross-stratified sandstone	Coarse-grained, occasionally pebbly sandstone. Bedforms are presented as either tabular or lenticular bodies.	Cross-stratified sandstone that possesses low-angle inclined beds with dips varying between 25° and 40°; in places mud drapes	Migration of straight-crested dunes in lower flow regime conditions (Collinson, 1996). Low-angle cross-stratified sandstone and pebbly sandstone are related to plane bed deposition during or close to the upper flow regime (Collinson, 1996). The occurrence of mud drapes is indicative of tidal influence during the deposition (Reineck & Wunderlich, 1968).	FA1, FA2, FA3, FA4, and FA5
F6: ripple cross-laminated sandstone	Fine- to medium-grained sandstone with moderate to well sorting and include mud laminae or mud drapes. Ripples are typically asymmetric and bimodal, and beds typically display a	Asymmetrically ripple cross-lamination, in few places wave-ripple lamination, and common mud-drapes	Migration of complex ripples corresponding to relatively weak currents during the lower flow regime (Stear, 1978). Asymmetrical and bimodal ripples indicate oscillatory periodic flow and flow	FA1, FA2, FA3, FA4, FA5, and FA6

(Continues)

**TABLE 1** (Continued)

Facies	Description	Sedimentary structures	Facies interpretation	Appearance
	lenticular shape and fine upwards.		reversal (Reineck & Wunderlich, 1968). Mud drapes suggest a tide-influenced depositional environment (Reineck & Wunderlich, 1968).	
F7: parallel-laminated sandstone	Fine- to coarse-grained sandstone with poor to moderate sorting. Beds are often tabular forming horizontal or very-low-angled lamination, typically 15° or less.	Parallel lamination and in places superimposed ripples	Plane bed deposition during or close to the upper flow regime that is too shallow to have been reworked into subcritical bedforms (Collinson, 1996).	FA1, FA2, FA3, FA4, and FA5
F8: hummocky/swaley cross-stratified sandstone	Medium-grained sandstone with both hummocky cross-stratification and swaley cross-stratification. Beds form in sheet-like, tabular morphologies with either erosional or sharp boundaries.	Long smile and frown-like structures in sandstone	Infilling of sand scours left as the result of oscillatory flows and unidirectional storm currents below the fair weather wave-base (Leckie & Walker, 1982).	FA3, FA4, FA5, and FA6
F9: heterolithic deposits	Fine- to medium-grained sandstone with interbedded mudstone exhibiting flaser, wavy, and lenticular bedding. Beds are tabular to lenticular with sharp or gradational bases. Heterolithic beds are occasionally inclined.	Horizontal, wavy, lenticular, and flaser lamination; in places mud drapes	Bedload transport during tidal flow and suspension settlement during slack-water periods, leading to observed cyclic mud and sand beds (Reineck & Wunderlich, 1968).	FA2, FA4, and FA5
F10: structureless mudstone	Light to dark grey mudstone that forms both lenticular and tabular beds with both gradational and sharp boundaries.	In places and very weak parallel lamination	Deposition of suspended sediments during low-energy periods (Bridge, 2006)	FA1, FA2, FA3, FA4, FA5, and FA6
F11: parallel-laminated mudstone	Light to dark grey mudstone that form both lenticular and tabular beds.	Thin horizontal lamination	Deposition through low-energy suspension, which is influenced by weak currents that rework the sediments into laminated units (Pontén & Plink-Björklund, 2007)	FA1, FA2, FA3, FA4, FA5, and FA6

environments, and sub-environments were defined from primary sedimentological features (lithology, sedimentary structures, and sedimentary textures), and shifts in palaeogeography were interpreted through variations in interpreted bathymetry within the stratigraphic column. Excellent exposures permitted the direct observation of stratal stacking patterns and the documentation of key surfaces within the SSB. The sequence stratigraphic model was developed from interpretation of detailed field data combined with the recognition of sequence stratigraphic surfaces. This integration of data allowed the identification of the building blocks of the sequence stratigraphic framework, such as depositional systems and systems tracts.

## 4 | SEDIMENTARY FACIES, FACIES ASSOCIATIONS, AND DEPOSITIONAL ENVIRONMENTS

Eleven facies (F1 to F11) have been identified in the examined section of the SSB and grouped into six facies associations (FA1 to FA6).

Facies associations were determined based on sedimentological and stratigraphic criteria (e.g., the perpendicular and horizontal facies assemblages and variations, the prevalent depositional process, as well as the geometry and position of major stratigraphic surfaces). The boundaries between successive facies associations usually coincide with formation boundaries but, in some instances, they are placed within formations. From bottom to top, the following facies associations were identified: (a) fluvial (FA1, WHF); (b) estuarine (FA2, PBF), upper shoreface (FA3, PBF), and lower-shoreface (FA4, PBF); (3) inner shelf (FA5, SPF); and (4) outer shelf (FA6, WS). The main facies characteristics are summarized in Table 1.

### 4.1 | FA1: fluvial (WHF)

#### 4.1.1 | Description

This sedimentary succession is approximately 70 m thick and is composed of interbedded sandstone, breccia, and conglomerate (Figure 4). The sandstone is fine- to very coarse-grained, thin- to very thick-bedded (0.1–1.5 m), and forms thick amalgamated units (up to

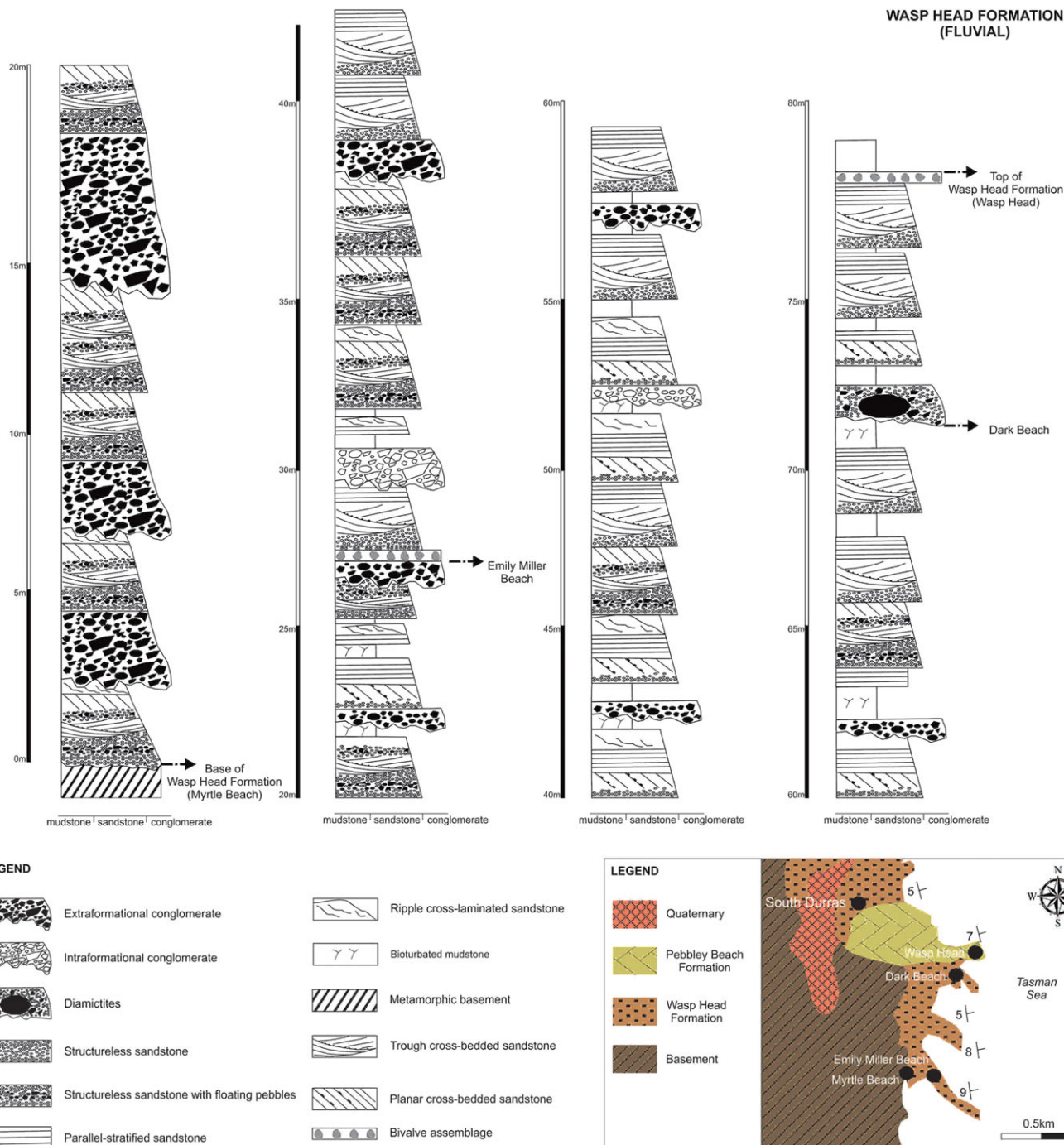


**FIGURE 4** Representative section of the Wasp Head Formation illustrating the sedimentology of the fluvial deposits. Note the fining-upward trend, indicative of a progressive decrease in energy with time [Colour figure can be viewed at [wileyonlinelibrary.com](http://wileyonlinelibrary.com)]

5 m thick). They are bounded by erosional surfaces that range from flat to concave-up and define thick (metre-scale) sedimentary units (Figure 5a). Internally, these units exhibit changes in thicknesses, grain size, and dip in the palaeoflow direction (eastwards). Mudstone beds are rare and usually thin-bedded although scarce, medium-bedded mudstone units are present. These beds are both structureless and parallel-laminated (F10 and F11).

Granule to boulder breccia (F1) forms beds up to 5 m thick and fines upward into coarse- to medium-grained sandstone (Figure 5b). The conglomerate displays erosional contacts with the underlying sandstone beds. The clasts include bullet-shaped forms with smooth and abraded stoss ends and plucked lee ends. Breccia is clast-

matrix-supported, oligomictic, disorganized, or with rare inverse to normal grading and clast imbrication. Conglomerate and sandstone units with intraformational clasts are also preserved (Figure 5c). They include fine- to coarse-grained sandy matrix with rounded to subangular sandstone and mudstone clasts that are 1–12 cm in diameter. Matrix-supported and poorly sorted conglomeratic layers are also present and include clasts up to boulder size, with subangular and sub-rounded shapes. They are relatively thin (<1 m), tabular, and laterally extensive, and their basal contact is erosional or deformed (Figure 5d). This type of conglomerate displays a wide range of clast roundness and a strong  $\alpha$ -axis fabric. The clasts are of mixed provenance including both intra- and extra-basinal clasts, and they develop

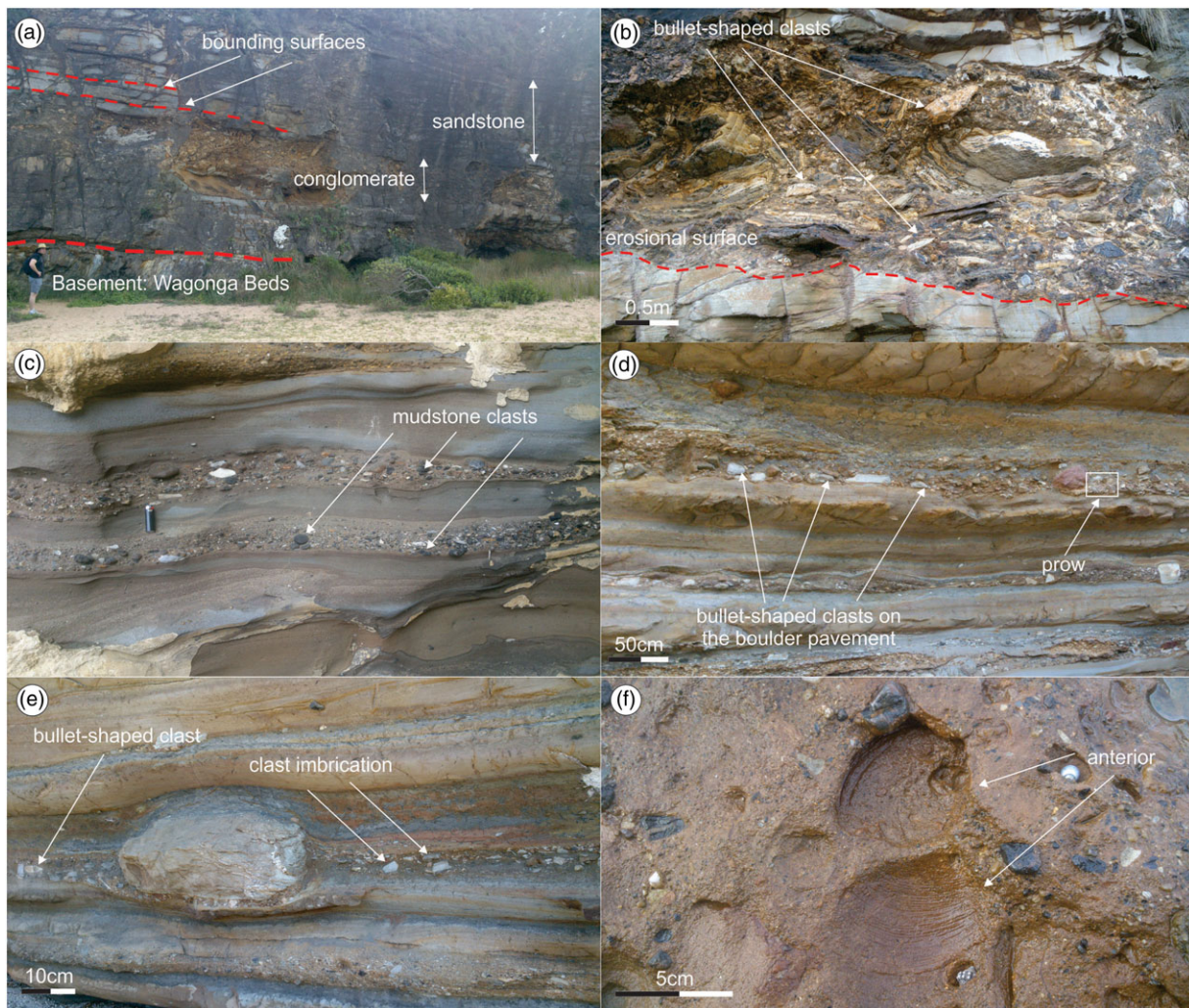


**FIGURE 5** Outcrop photographs illustrating diagnostic features of the fluvial deposits in the southern Sydney Basin. (a) Repetition of coarse-grained sandstone and conglomerate (Myrtle Beach). (b) Close-up view of the conglomeratic beds. Note the bullet-shaped clasts that imply a glacially influenced river system (Myrtle Beach). (c) Intraformational conglomerate with abundant mudstone clasts (Emily Miller Beach). (d) and (e) Diamictites with characteristic prows, bullet-shaped clasts, and clast imbrication that indicate transport in the basal traction zone (Dark and Emily Miller Beach, respectively). (f) Bivalve population that exhibit symmetrical sculpture and anterior thickening (Wasp Head). Person for scale is 180 cm tall [Colour figure can be viewed at [wileyonlinelibrary.com](http://wileyonlinelibrary.com)]

a boulder pavement. Some of the boulders have well-developed stoss and lee sides, as well as frontal sediment pows (Figure 5e). The clasts exhibit imbrication and are often bullet-shaped. Rare bivalve populations that lack association with marine invertebrates (e.g., brachiopods) occur. These bivalves exhibit symmetrical sculpture and anterior thickening (Figure 5f). They also lack evenly spaced radial concentric ribs, as well as repair breakings (Figure 6a).

The interbedded sandstone is often structureless (F2) and develops thick amalgamated sets (up to 5 m thick). These sets often have parallel stratified floating large clasts, and their grain sizes range from very coarse- to fine-grained sandstone (Figure 6b). Thin to medium conglomeratic layers (a few centimetres thick) may occur at the base of tabular (F5) and trough cross-bedded sandstone (F3). The trough sets are abundant, and a few centimetres to tens of centimetres thick (Figure 6c). Tabular cross-bedding is less abundant but still common. Alternating foresets of sandstone and conglomerate within cross-bedded sets are present (Figure 6d). Trough cross-bedded, pebbly sandstone (F3) is also present, composed of fine- to medium-grained,

cross-bedded pebbly sandstone with abundant rounded pebble-grade extraclasts (Figure 6e). Pebbles range in diameter from 15 to 40 mm. Parallel stratified sandstone (F7) is of minor appearance and, when present, is fine-grained and with well-defined horizontal stratification. Trough cross-laminated sandstone (F6) is present and occurs commonly towards the top of the beds, along with parallel-laminated sandstone (Figure 6f). Structureless sandstone (F2) also occurs as tabular beds.

This succession exhibits a fining-upward trend (Figure 4). At the base, usually structureless thick-bedded sandstone with floating large clasts is intercalated with thick breccia beds forming stacked multistorey sheets. These sheets become sandier up-sequence and consist of planar (F5) and trough cross-bedded sandstone (F3), with scarce and thinner-bedded conglomerate. They eventually evolve up-sequence into a sand-dominated unit consisting of both trough cross-bedded (F3) and planar cross-stratified sandstone (F5). The frequency and thickness of mudstone increases up-sequence and the upper parts of this sedimentary succession contain medium-bedded mudstone (F10 and F11), interbedded with thick-bedded sandstone.

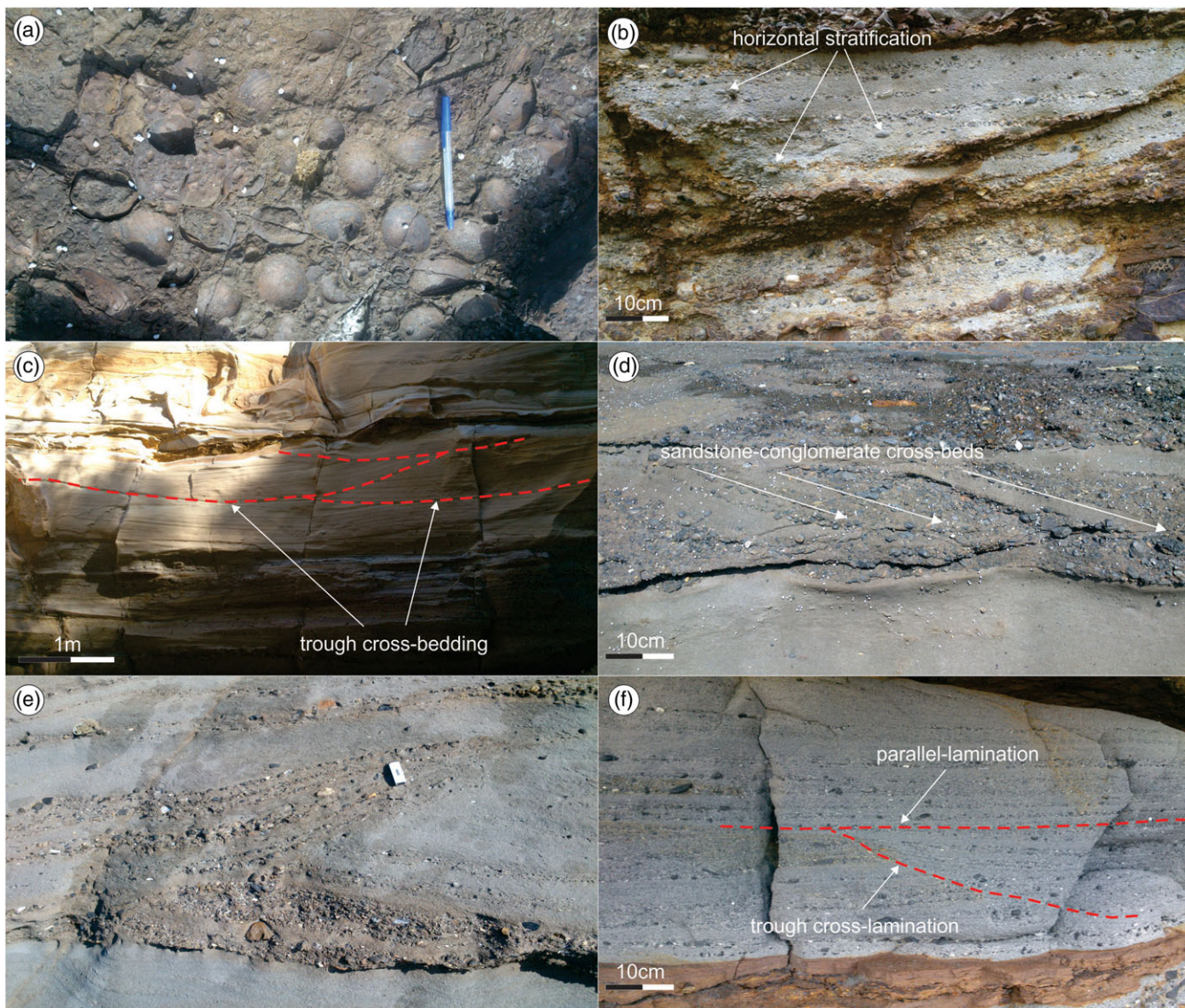


**FIGURE 6** Outcrop photographs illustrating diagnostic features of the fluvial deposits in the southern Sydney Basin. (a) Bivalve populations that lack of traits that confer resistance to predation or enhance stability of the shell in the sediment (Emily Miller Beach). (b) Coarse-grained sandstone with parallel-stratified floating pebbles (Myrtle Beach). (c) Large-scale trough cross-stratified sandstone units (Dark Beach). (d) Cross-bedded sandstone with alternating foresets of sandstone and conglomerate within cross-bedded (Myrtle Beach). (e) Trough cross-bedded, pebbly sandstone. Note the abundant rounded pebble-grade extraclasts (Dark Beach). (f) Trough cross-laminated sandstone at the top of the beds, along with parallel-laminated sandstone (Myrtle Beach). Pen for scale is 15 cm long [Colour figure can be viewed at [wileyonlinelibrary.com](http://wileyonlinelibrary.com)]

Palaeocurrent directions, collected from cross-stratification and clast imbrications in the WHF, display a generally consistent pattern of transport and indicate an easterly flow direction (Fielding et al., 2006).

#### 4.1.2 | Interpretation

This sedimentary succession is interpreted here as a fluvial system. The clast-supported conglomerate and sandstone with floating larger clasts record bedload deposition from stream flows (Nemec & Postma, 1993). Horizontal stratification suggests deposition on near-horizontal pavements, either the tops of braid bars or as lags on channel floors (Nemec & Postma, 1993). Channel conglomerate bodies that fine upwards into sandstone suggest either gradual diminution of flow through diversion or systematic lateral migration of a curved channel reach (Bridge, 2006; Collinson, 1996). Clast imbrication

points at tractional deposition (Whiting, Dietrich, Leopold, Drake, & Shreve, 1988) and in conjunction with the bullet-shaped clasts could be associated to a glacially influenced river system (Arnaud & Etienne, 2011). The bounding surfaces that dip towards the palaeoflow direction can be related to downstream accretion elements (Miall, 1977) and suggest repeated flood events and macroform aggradation (Magalhães, Scherer, Raja Gabaglia, Ballico, & Catuneanu, 2014). Conglomeratic units at the base of both parallel and trough cross-bedded sandstone are interpreted here as channel lag deposits that represent the coarsest sediment fraction transported by the flow during high-energy conditions. The intraformational conglomerate is most likely the result of localized reworking of sandstone and mudstone beds, with clasts derived either via erosion from the base of the channel or from bank collapse at the channel margin. Sandstone beds predominate in the upper parts of the channels, which could be related to the

decrease in channel capacity heralding the abandonment phase (Bridge, 2003).

The matrix-supported and poorly sorted conglomerate with bullet-shaped clasts and clast imbrication is interpreted here as diamictite. It suggests transport in the basal traction zone and provides evidence for a glaciogenic influence on sedimentation (Arnaud & Etienne, 2011). The frontal sediment prows indicate clast ploughing through the soft, deformable bed (Clark & Hansel, 1989). The enlargement of sediment prows most likely led to increased resistance that eventually outpaced the force exerted on the clasts by ice flow causing clast lodgement (Evans, Phillips, Hiemstra, & Auton, 2006). The clasts with well-developed stoss and lee sides and strong  $\alpha$ -axis fabric could be related to constrained shear at ice-till interface, low-density of the clasts, and drag imposed by ice and matrix (Evans et al., 2006). The matrix-supported nature of the conglomerate most likely facilitated the clast rotation and their alignment within the direction of shear. Erosional contacts with the underlying sandstone beds are interpreted as the result of syndepositionally sheared till, which is associated to intense shear in the basal zone (Piotrowski, 1994). These field observations indicate a lodgment and deformation tillite (according to the classification of Arnaud & Etienne, 2011). Their association with laminated and/or massive mudstone can be ascribed to a glacially influenced fluviacustrine depositional setting.

Trough cross-bedded sandstone is the product of migrating three-dimensional dunes, whereas tabular sets are produced by straight-crested dunes within the context of a lower flow regime (Collinson, 1996). Cross-stratified pebbly sandstone is interpreted as the result of migration and deposition of sandy barforms within a fluvial channel representing downstream accretion under conditions of lower flow regime (Medici, Boulesteix, Mountney, West, & Odling, 2015). Alternating foresets of conglomerate and sandstone in the cross-bedded sets reflect discharge fluctuations (Steel & Thompson, 1983). Parallel-laminated sandstone represents migration of bedforms during upper flow regime conditions (Collinson, 1996; Magalhães et al., 2014). Cross-laminated sandstone is interpreted as reflecting relatively weak currents during the lower flow regime (Stear, 1978). The association of trough cross-stratification with parallel lamination, especially in the lower parts of sandstone beds, records fluctuations in flow stage and/or sediment concentration during flood events (Bridge, 2006). Nevertheless, the prevalence of trough cross-bedding indicates a relatively steady discharge. Structureless sandstone at the base of channel sandbodies is ascribed to rapid deposition during floods (Collinson, 1996; McCabe, 1977).

The general lack of overbank fines and the almost entirely amalgamated nature of the sandstone beds indicate deposition in the proximal fluvial channel area and recurrent cut-and-fill processes (Collinson, 1996; Nichols & Fisher, 2007). This indicates channel mobility and lateral migration and reworking of the adjacent floodplain deposits or repeated avulsion to new positions on the proximal floodplain area (Nichols & Fisher, 2007). The fining-upward trend suggests a progressive decrease in energy with time that can be related to the decrease in slope gradient of the fluvial systems and an increase in the rate of base-level rise (Catuneanu, 2006). The observed characteristics in the bivalve populations indicate that predation and shell breakage have been of little evolutionary imperative (Vermeij & Dudley,

1985). The lack of recording evidence of marine predators and traits that imply resistance to predation or enhanced stability of the shell in the sediment, in conjunction with their association with large-scale trough cross-bedding suggests the freshwater origin of the bivalves.

## 4.2 | FA2: estuarine system (PBF)

### 4.2.1 | Description

This sedimentary succession is approximately 90 m thick and laterally extensive. It consists of sandstone and mudstone that form two thickening- and coarsening-upwards cycles (Figures 7–9a). The lower cycle is 45 m thick and is composed of a mudstone-dominated unit (15 m thick) that is overlain by a sandstone-dominated unit (30 m thick). The mudstone-dominated unit is composed of structureless mudstone (F10), nevertheless parallel-laminated mudstone (F11) and heterolithic strata (F9, lenticular bedding) are also present. The interbedded sandstone beds are thin- to thick-bedded (0.2–1 m) and structureless (F2) or parallel-laminated (F7) (Figure 9b). Furthermore, some of the sandstone beds display mud drapes, oscillation ripple lamination (F6), and low-angle undulatory parallel lamination (F8, micro-hummocky cross-stratification [HCS]; Figure 9c). Trace-fossil suites that are composed of sharp-walled, unlined, dwelling burrows occur. The overlying sandstone-dominated part is composed of parallel-laminated (F7), planar cross-bedded (F5), and HCS sandstone (F8), which is interbedded with thin- to medium-bedded (0.1–50 cm) mudstone layers (F10 and F11; Figure 9d). Mud drapes and heterolithic strata (mostly flaser bedding) is common throughout this unit.

The upper cycle is composed of a thick muddy part (6 m thick) that is overlain by a sandstone-dominated interval (25 m thick). In the thick muddy unit (F10 and F11), rare fine-grained, thin- to medium-bedded (0.05–0.2 m), and ripple cross-laminated sandstone (F6) also occur (Figure 10a). The overlying sandstone-dominated part is composed of structureless (F2), parallel-laminated (F7), and ripple-cross-laminated (F6), very coarse- to very fine-grained sandstone. These deposits often rest on an erosional surface and display a fining-upward trend. At the base, basal sandstone deposits evolve upward into intercalations of sandstone and mudstone, in the form of heterolithic beds (F9). The heterolithic beds form both sand- and mud-dominated packages that are 0.4–2 m thick and separated by low-angle (5°–10°) inclined surfaces (Figure 10b). These packages can be distinguished based on the relative abundance of flaser and lenticular bedding, respectively, whereas packages with equal sandstone-mudstone contents (wavy bedding) occur. Internally, the heterolithic beds comprise 5–20 cm thick sand- to mud-dominated couplets. The sandy parts contain current ripple cross-lamination, and the ripples often dip in opposite directions. The mud-dominated couplets are mostly structureless or parallel-laminated and may include very thin-bedded sandstone in the form of lenticular- to wavy-bedding. Millimetre- to centimetre-thick mud drapes are the most characteristic feature in this facies association. Heterolithic beds are either inclined or sheet-like. The inclined counterparts contain reactivation surfaces marked by the interruption of cross-strata with the same direction (north-northwest-directed) and inclination above and below (Figure 10c). Mud drapes and soft-sediment deformation structures (slumps) occur. Thicker-bedded (1–2 m thick), sand-dominated intervals are rare but comprise bipolar

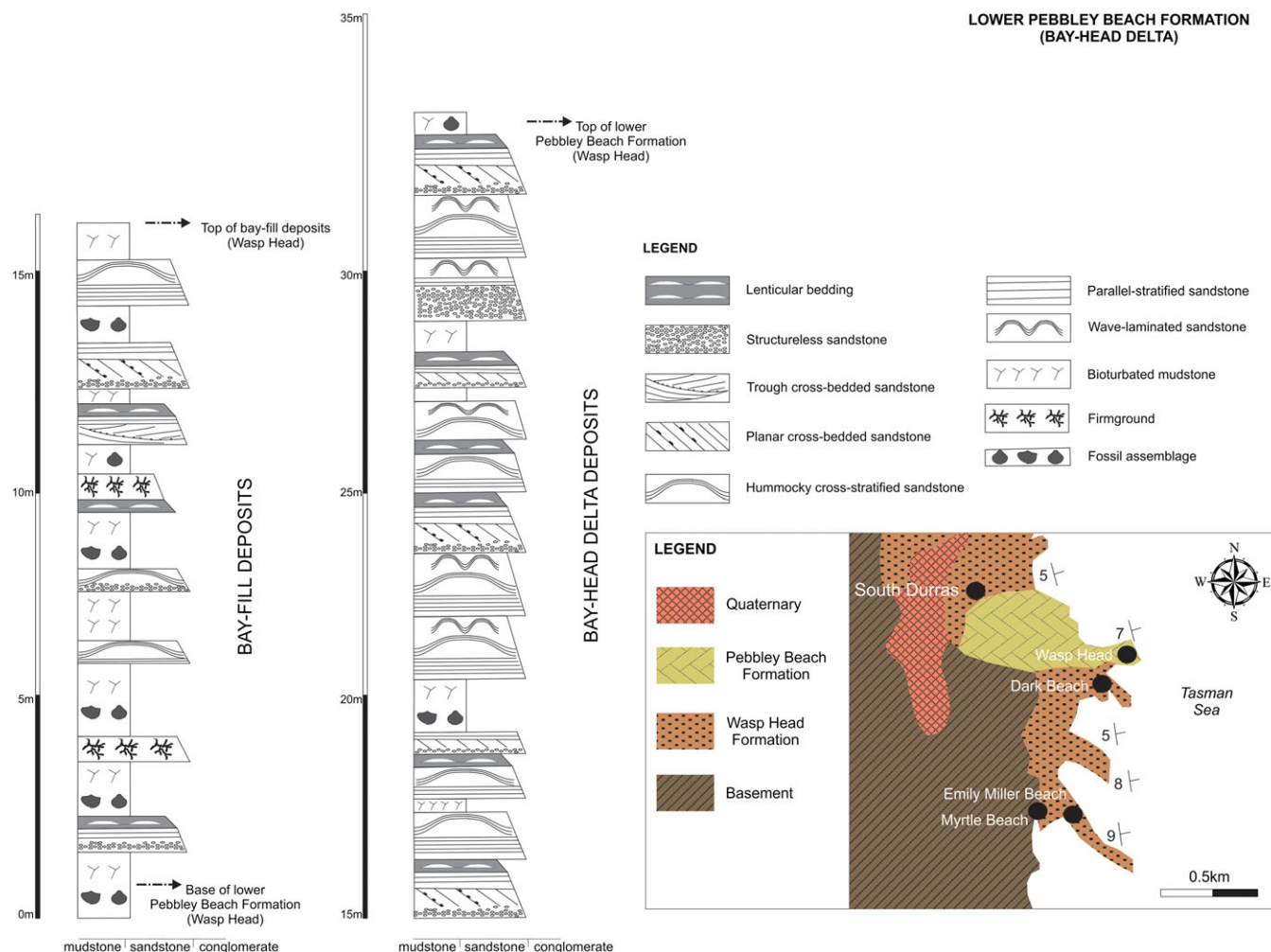


**FIGURE 7** Representative section of the lower Pebbley Beach Formation that depicts the sedimentological characteristics of the bay-head delta deposits. Note the progradation of the bay-head delta deposits over the bay-fill delta sediments [Colour figure can be viewed at [wileyonlinelibrary.com](http://wileyonlinelibrary.com)]

(SW- to NE-directed), trough, and planar cross-bedded sandstone (F3 and F5) (Figure 10d and 10e). Trace fossils assemblages are composed of *Cruziana-Skolithos* ichnofacies and contain cylindrical to subcylindrical, straight to curved, vertical to subvertical, unbranched burrows (Figure 10f). Body fossils from marine invertebrates (e.g., brachiopods) occur. Palaeocurrent data from the PBF suggest a bimodal distribution, with a significant south-westward and a less important eastward trend (Fielding et al., 2006; Rygel et al., 2008a).

#### 4.2.2 | Interpretation

This depositional system is interpreted as estuarine with its associated "bay-head" delta (basal thickening and coarsening-upwards cycle), central estuary, tidal channels, and tidal flats (upper thickening and coarsening upwards cycle). In the basal cycle, the upward transition from the heterolithic and overall mudstone-rich assemblage into the sandstone-rich assemblage is interpreted as the result of the progradation of a sand-depositing system over bay deposits (Plint & Wadsworth, 2003). In the SSB, bay-head delta deposits form a coarsening-upwards unit within a transgressive interval representing prodelta lithofacies (bay-fill deposits) that are overlapped by sandy bay-head delta deposits. Structureless mudstone is considered as deposits that

accumulated during periods of low energy and associated suspension fallout, whereas the weak lamination is ascribed to the regular inundation by currents (Bridge, 2006; Maravelis, Konstantopoulos, Pantopoulos, & Zelilidis, 2007). Parallel-laminated mudstone is ascribed to deposition through low-energy suspension, which is influenced by weak currents that rework the sediments into laminated units (Pontén & Plink-Björklund, 2007). The trace-fossil suites that consist of sharp-walled, unlined, dwelling burrows are interpreted as firmgrounds and are associated with sediment that undergone burial, compaction, and dewatering (Gingras, Pemberton, & Saunders, 2000). Structureless sandstone is interpreted here as the deposits of high-density flows and indicate high sedimentation rates (Lowe, 1988; Magalhães, Scherer, Raja Gabaglia, & Catuneanu, 2015). The presence of mud drapes and heterolithic bedding is indicative of tidal influence during the deposition (Reineck & Wunderlich, 1968). Sandstone beds with oscillation ripple lamination and low-angle undulatory parallel lamination are interpreted as storm-related events in the bay-head delta (Joeckel & Korus, 2012).

In the upper cycle, the central estuary sediments are represented by thick muddy successions. Their occurrence indicates that fair-weather waves and storm waves have been less effective at reworking the substrate (Gingras et al., 2012). The sand interbeds

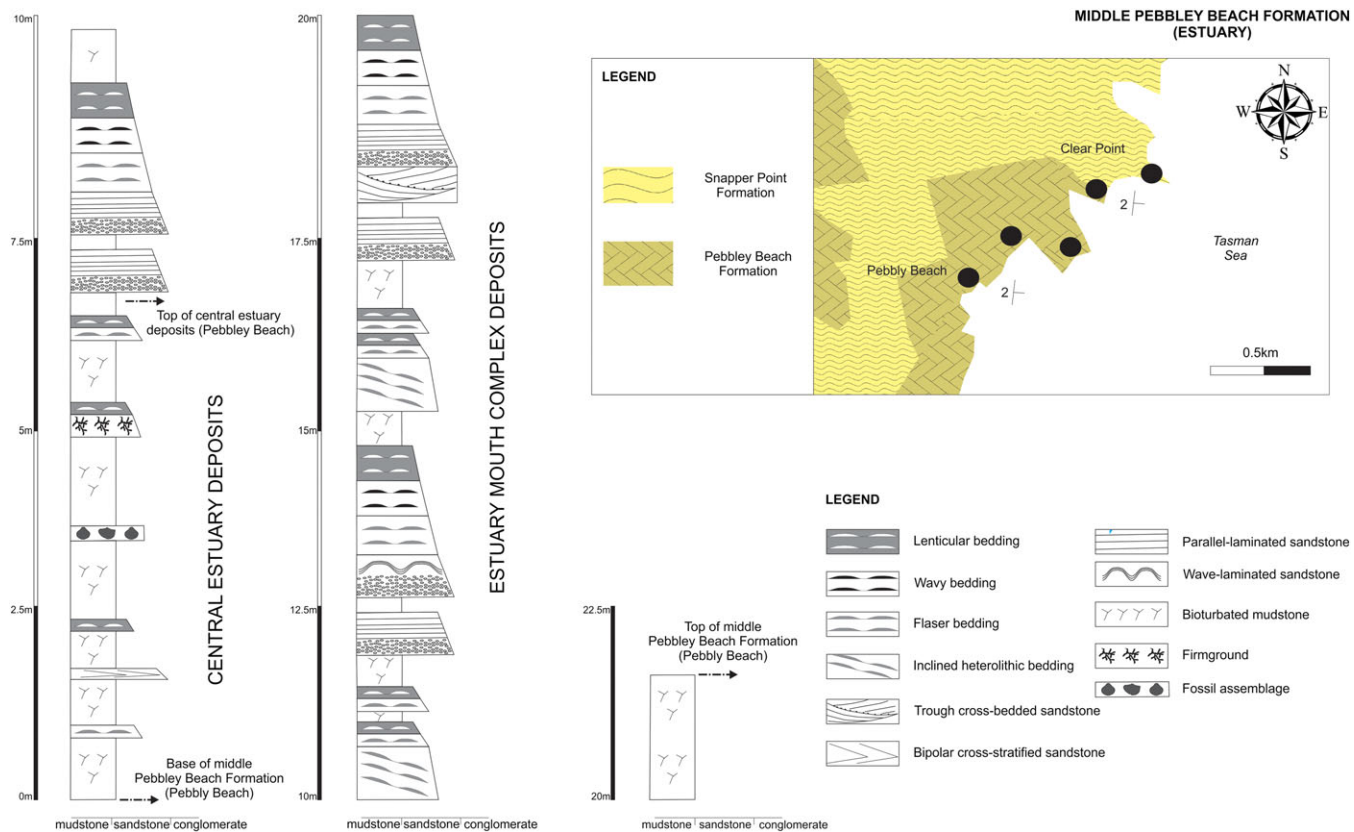


**FIGURE 8** Representative section of the middle Pebbley Beach Formation that depicts the sedimentological characteristics of the estuarine deposits. Note the coarsening-upwards trend from the mud-dominated central estuary facies to the sand-rich deposits of the estuary-mouth complex [Colour figure can be viewed at [wileyonlinelibrary.com](http://wileyonlinelibrary.com)]

may have been deposited during river-flood events, based on the predominance of current ripples (Gingras et al., 2012). Bedload transport during tidal flow and suspension settlement during slack-water periods are indicated by alternating flaser and wavy bedding (Reineck & Wunderlich, 1968). In the upper cycle, the sand-rich unit is interpreted as estuary-mouth complex deposits. The sandy intervals with the fining-upward trend are consistent with channelized deposits, whereas the overlying sheet-like heterolithic beds are considered to be deposits within a non-channelized and relatively unconfined setting, under the influence of tidal currents. Reactivation surfaces and cross-lamination dipping in opposite directions suggest tidal influence and flow reversal. Reactivation surfaces are representative of subtidal, tidal-influenced environments such as channels (Bowman & Johnson, 2013). The geometry of the inclined-heterolithic beds suggests barforms with straight accretion surfaces such as elongate side-attached or mid-channel bars (Legler et al., 2013). The soft-sediment deformation structures suggest downslope movement of sediment across bar slopes (Legler et al., 2013). Repetitions of millimetre- to centimetre-thick layers of sandstone and mudstone in the inclined-heterolithic beds suggest deposition in a highly fluctuating hydraulic regime (Legler et al., 2013; Olariu, Olariu, Steel, Dalrymple, & Martinus, 2012). Sheet-like heterolithic beds are considered to be deposits within a non-channelized and relatively unconfined setting, under the influence of tidal currents. The low-diversity occurrence of *Cruziana-Skolithos* ichnofacies indicates that food resources were present but the moderate colonization by invertebrates implies considerable physical and chemical stress, such as high

sedimentation rates, low salinities, and oxygen deficiencies (Gingras, MacEachern, & Dashtgard, 2011).

### 4.3 | FA3: upper shoreface (PBF)

#### 4.3.1 | Description

These sedimentary strata is approximately 5 m thick and consists of sharp-based, medium- to thick-bedded (0.3–1 m) and often amalgamated (up to 3 m thick) sandstone (Figure 11). Mudstone beds are rare and very thin-bedded (a few centimetres thick) (F10 and F11). The upper bed surfaces of the sandstone may be sharply overlain by, or gradually pass upwards into, mudstone (Figure 12a) or may be flat, undulose, or wave rippled (F6). Parallel-laminated sandstone (F7) occurs (Figure 12a and 12d). HCS and swaley cross-stratification (SCS) occur, in the form of medium- to large-scale cross-stratification (F8), in which the undulating and gently dipping laminae preserve a three-dimensional bedform comprising large amplitude (1–5 m), low relief (0.1–0.5 m) hummocks and troughs (Figure 12b and 12c). HCS consists of a basal planar to low-angle laminated unit (1 to 5 cm thick) and is overlain by an undulose basal scour surface. Convex and concave laminations have long wavelength and drape, downlap, or onlap the basal scour surface (Figure 12b and 12d). Oscillatory ripple cross-lamination (F6) often occurs at the tops of these sandstone beds. Bivalve concentrations are also preserved and contain randomly oriented, fragmented shells that form beds up to 30 cm thick (Figure 12e). These beds are accumulated at the top of the upper

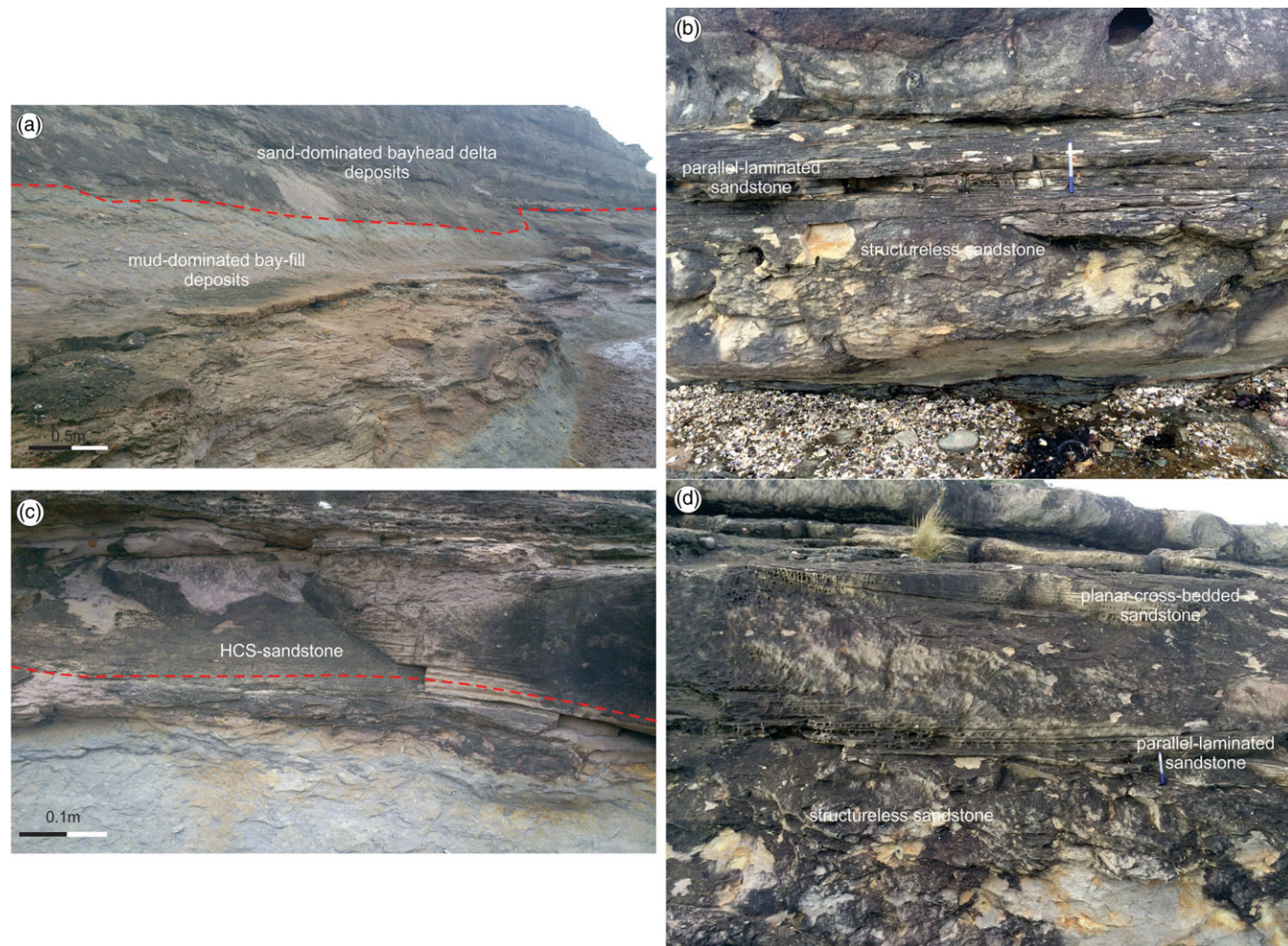


**FIGURE 9** Outcrop photographs illustrating diagnostic features of the bay-head delta deposits in the southern Sydney Basin. (a) Progradation of bay-head delta deposits over bay fill deposits and associated thickening and coarsening-upward trend (Wasp Head). (b) Structureless sandstone overlain by parallel-laminated sandstone (Wasp Head). (c) Storm-associated sandy units in bay-head delta (Wasp Head). (d) Sandstone bed with parallel and planar cross-stratification (Wasp Head). HCS = hummocky cross-stratification [Colour figure can be viewed at [wileyonlinelibrary.com](http://wileyonlinelibrary.com)]

shoreface deposits. Bioturbation is rare and restricted to the upper parts of some of the sandstone beds (Figure 12f).

#### 4.3.2 | Interpretation

Shoreface deposits are conceptually regarded as entirely wave-dominated (Dalrymple et al., 1992), but the ancient shoreface deposits are also affected by tides (Dashtgard, Gingras, & MacEachern, 2009). The shoreface depositional model is well established in the geological literature (e.g., Reading & Collinson, 1996; Walker & Plint, 1992), but shoreface deposits are present in a wide range of coastal settings, and thus, their sedimentological characteristics are highly variable (Dashtgard et al., 2009). The upper shoreface is dominated by trough and planar cross-stratification, but with increasing storm-wave influence, sedimentary structures produced by storm waves (HCS and SCS) are increasingly dominant (Ainsworth, Flint, & Howell, 2008). These considerations and the recorded sedimentological evidence indicate that the studied sedimentary succession represents upper shoreface deposits. The HCS and SCS have been interpreted to record storm-related deposition (Leckie & Walker, 1982). The coexistence of undulating lamination and scours is most likely ascribed to deposition

under waning combined flow conditions (Dumas & Arnott, 2006). Scours reflect periods of variation in storm intensity. They can be also produced by instantaneous increases in shear strength caused locally as a result of the interaction of wave currents and offshore-directed unidirectional storm currents (Dumas & Arnott, 2006; Scott, 1992). The beds with low-angle lamination infilling scours are typical of periods of lower rates of aggradation when swales rather than hummocks are preserved (Dumas & Arnott, 2006). Wave ripples in the upper parts of beds indicate either wave reworking during the waning stage of a storm or later fair-weather wave reworking (Bowman & Johnson, 2013). The very rare preservation of mudstone units in thick HCS- and SCS-dominated successions indicates a high-energy shoreface environment.

It is regarded that SCS and HCS form at the same time, potentially during the same storm event, but in different water depths. In particular, SCS is thought to form in shallower water (e.g., shoreface), whereas HCS is a sedimentary structure diagnostic of deeper water (e.g., inner shelf) (Dott & Bourgeois, 1982; Dumas & Arnott, 2006; Sageman, 1996). Recently published investigation of Peters and Loss (2012) challenges this discrimination and indicates that based upon the wave height distributions, sedimentary structures cannot be attributed to

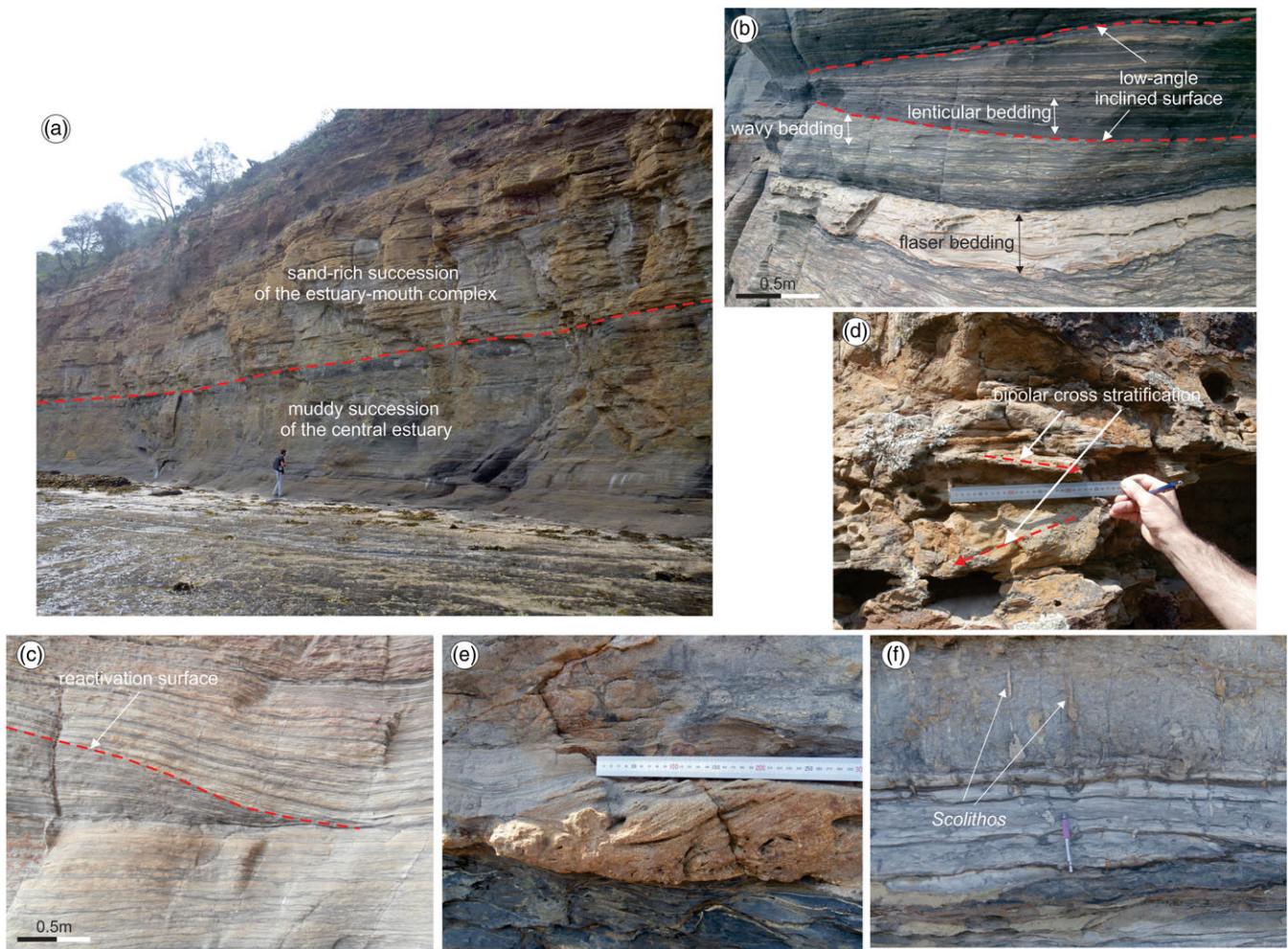


**FIGURE 10** Outcrop photographs illustrating diagnostic features of the estuarine deposits in the southern Sydney Basin. (a) Thick muddy successions in the central estuary (Pebbly Beach). (b) Flaser to lenticular heterolithic bedding, bounded by low-angle surfaces (Pebbly Beach). (c) Reactivation surface (point-bar setting) (Pebbly Beach). (d) Bipolar (herringbone) cross-stratification that implies formation by traction and suspension with tidal influence (Pebbly Beach). (e) Current ripple cross-lamination (Pebbly Beach). (f) Vertical burrows (*Scolithos*) implying high-sedimentation rates. Person for scale is 180 cm tall, ruler is 30 cm long, and pen is 15 cm long (Pebbly Beach) [Colour figure can be viewed at [wileyonlinelibrary.com](http://wileyonlinelibrary.com)]

water depth, but are associated with the physical properties of sediment and the flow type (oscillatory vs. combined flow). This work also suggests the absence of any clear relationship between wave size and hydrodynamic state (oscillatory vs. combined flow), highlighting that HCS and SCS can form in both shoreface and shelf settings, but with a continuously decreasing probability of preservation in shallower water (shoreface). This is in agreement with outcrop-based case studies in both ancient (Dashtgard, Frey, & MacEachern, 2012; Løseth, Steel, Crabaugh, & Schellpeper, 2006; Rossi & Steel, 2016) and modern settings (Budillon, Vicinanza, Ferrante, & Iorio, 2006; Keen et al., 2006) that have documented HCS in the shoreface. The lack of mudstone beds and bioturbation is consistent with deposition in a storm-related, high-energy depositional environment (MacEachern & Bann, 2008; Pemberton et al., 2002). Shell beds are interpreted as condensed sections that have been accumulated in a high-energy setting, as suggested by the chaotic arrangement of the shells. These shell beds are thought to have been accumulated due to repeating storm events in conditions of low net deposition (Kidwell, 1991; Zecchin & Catuneanu, 2013).

#### 4.4 | FA4: lower shoreface (PBF)

##### 4.4.1 | Description

These sedimentary strata form a unit that is approximately 15 m thick (Figure 11) and laterally extensive (up to hundreds of metres). It is typified by sub-horizontal or very low-angle depositional dips. This unit is lithologically highly variable and dominated by heterolithic bedding (F8) including lenticular-bedded mudstone, wavy-bedded very fine-to-fine-grained sandstone, and often flaser bedding (Figure 13a). Internally, these ripples have opposite dip directions in adjacent sets (SW-NE). These ripples are usually asymmetric and round-crested displaying a biconvex profile and a convex-up sigmoidal profile (Figure 13b). Nevertheless, they are often symmetric displaying concave-up flanks, sharp crests, and broad troughs (Figure 13b). The majority of this facies comprises thin-bedded sandstone, with occasional medium- to thick-bedded (0.3–0.6 m), medium- to very coarse-grained sandstone. These thicker beds display cross-bedding (centimetre-scale) with rhythmically intercalated, thinner (millimetre-scale) mudstone layers. They exhibit diverge palaeocurrent directions

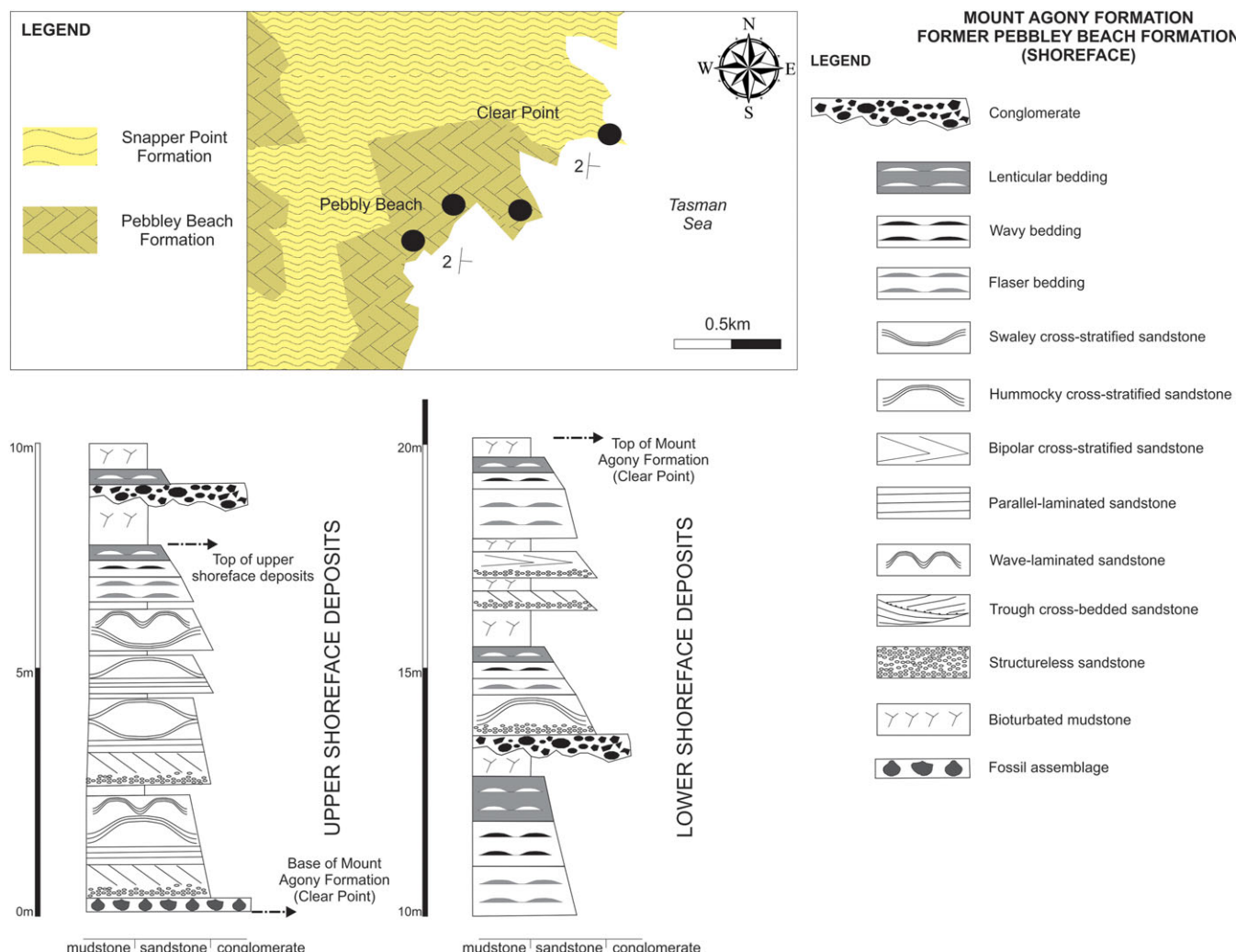


**FIGURE 11** Representative section of the upper Pebbley Beach Formation illustrating the sedimentological features of the shoreface deposits. Note the transition from upper to lower shoreface facies and the absence of middle shoreface deposits [Colour figure can be viewed at [wileyonlinelibrary.com](http://wileyonlinelibrary.com)]

towards the west-southwest (inferred flood-tidal direction; Figure 13c) and east-northeast (inferred ebb-tidal direction; Figure 13d). Sandstone beds with HCS (F8) occur and are associated with erosional discontinuities at the base of amalgamated (up to 1 m thick) hummocky cross-stratified beds (Figure 13e). They display a discrete increase in sand supply and enhanced bed amalgamation. Very thick-bedded sandstone (over 1 m thick) is rare and is organized into trough (F3) and sigmoidal cross-stratification (F4) (Figure 13f). Rip-up clasts occur at the base of the trough cross-beds. Towards the top, the cross-beds become thinner, and the sandstone evolves upwards into flaser, wavy, and lenticular bedding. Asymmetric and symmetric ripples (F6), planar cross-bedding (F5), and HCS (F8) are often interbedded with one another across these deposits (Figure 13b, 13c, and 13e). In medium-to coarse-grained sandstone, symmetric ripples and possible HCS are intercalated with onshore-directed (west-southwest-directed) planar cross-bedding. Conglomeratic layers (F1) are thin (a few cm thick) but present and are associated with scour surfaces. They occur either as isolated layers that are surrounded by mudstone or at the base of some of the medium-bedded, medium- to coarse-grained sandstone beds (Figure 13e).

Glendonites, mineral pseudomorphs after ikaite, a mineral that forms in cold (0–7°C) marine sediments, are present (Fielding et al., 2006). Ichnologically, this sedimentary succession includes a diverse mixture of deposit-feeding and grazing structures representing the distal expression of the *Cruziana* ichnofacies (Fielding et al., 2006). Vertical structures are less common and correspond to the archetypal *Cruziana* ichnofacies. Vertical burrows belong to the *Skolithos* ichnofacies (Fielding et al., 2006).

#### 4.4.2 | Interpretation

These deposits are interpreted as lower shoreface. The presence of sedimentary structures such as heterolithic bedding, mud drapes within cross-lamination, and herringbone cross-stratification suggests a tide-dominated depositional environment (Dalrymple & Choi, 2007; Legler et al., 2013). Heterolithic bedding is interpreted to have formed under highly fluctuating hydrodynamic conditions and indicates an alternation of tractional and suspension-settling processes, which is consistent with the action of tides (Collinson & Thompson, 1989). The asymmetric, round-crested ripples can be associated to



**FIGURE 12** Characteristics of storm-influenced upper shoreface deposits in the southern Sydney Basin (Pebbly Beach). (a) Sharp-based, planar cross-stratified sandstone that evolves upwards into mudstone. (b) Hummocky cross-stratification-dominated and (c) southern Sydney Basin-dominated shoreface sandstone. (d) Fine-grained sandstone with a basal planar to low-angle laminated unit overlying by an undulose basal scour surface. (e) Dismembered storm-related shell accumulations. (f) Rare trace fossils in shoreface sandstone. Pen for scale is 15 cm long [Colour figure can be viewed at [wileyonlinelibrary.com](http://wileyonlinelibrary.com)]

combined-flow structures, result of the combination of oscillatory and unidirectional flows (Dumas, Arnott, & Southard, 2005), whereas the symmetric, sharp-crested equivalents are interpreted here as oscillatory-flow features.

Tidal cross-bedding is the product of large flow-transverse bedforms (sand waves or medium to very large subaqueous dunes) and forms one of the best known ancient subtidal sandstone facies (Reading & Collinson, 1996). Cross-bedded sandstone is deposited during high tidal flow and mud layers during slack-water periods. Their presence suggests tide-influenced depositional environment (Visser, 1980). Sigmoidal internal strata form when bedforms with a concave

lee slope climb at relatively high angles such that the erosional bounding surface passes close to the bedform crest (Allen, 1982; Yokokawa, Masuda, & Endo, 1995). This structure is well developed by bedforms with long crests and relatively short lee faces. The erosional discontinuities can be ascribed to erosion, lowering of storm wave base, and an increase in storm wave energy that enhanced bed amalgamation (Hampson & Storms, 2003; MacEachern, Raychaudhuri, & Pemberton, 1992). The initial erosion is followed by abrupt infill by sand-rich flows (Bowman & Johnson, 2013). The overlying sandstone with HCS has been interpreted as storm-influenced deposition, common in shoreface to inner shelf depositional environments

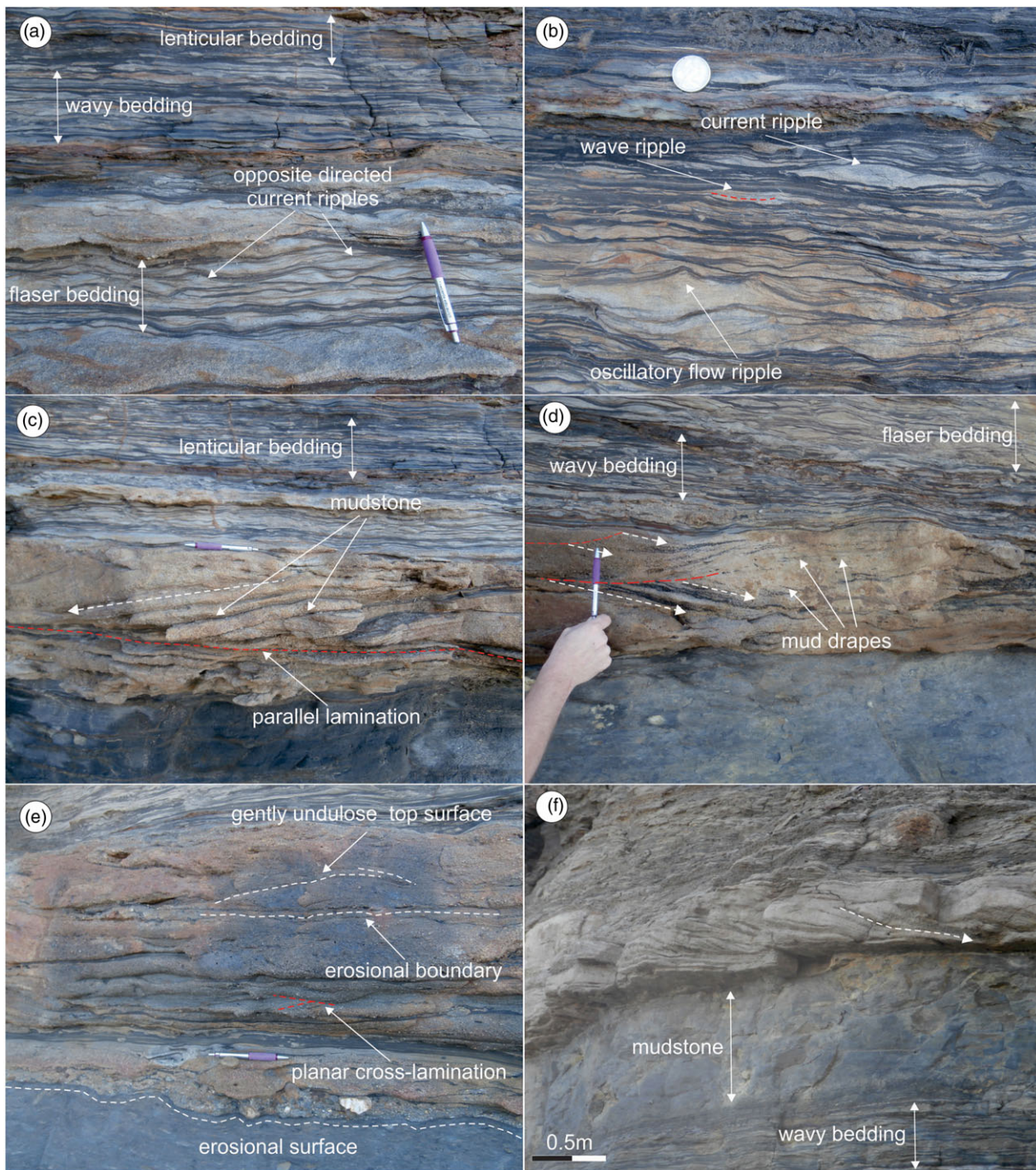


**FIGURE 13** Characteristic structures of the lower shoreface environment in the southern Sydney Basin (Clear Point). (a) Sheet-like, fining-upward flaser to lenticular heterolithic unit. (b) Cross-bedded sandstone with intercalated mud drapes and foreset, all showing a consistent palaeocurrent direction towards the west-southwest. (c) Cross-bedded sandstone with intercalated mud drapes and foreset, all showing a consistent palaeocurrent direction towards the east-northeast. The cross-bedded sandstone is overlain by gradationally bounded alternations of flaser to wavy bedding. (d) Medium to thick-bedded sandstone with sigmoidal cross-stratification, showing cross-beds downlapping over a thick muddy unit. (e) Erosional discontinuity recording lowering of storm wave base and increase in storm wave energy. (f) Wavy bedding that evolves upward in muddy unit with vertical burrows. Pen for scale is 15 cm long [Colour figure can be viewed at [wileyonlinelibrary.com](http://wileyonlinelibrary.com)]

(Peters & Loss, 2012; Rossi & Steel, 2016). These beds are interpreted to represent lower shoreface deposits recording the transport and redeposition of sand from upper shoreface sand-rich setting by large storms. The conglomeratic layers are interpreted here as individual storm events (tempestites). The isolated layers that are interbedded with mudstone most likely correspond to proximal tempestites representing the period when the storm is at its peak strength

(Nichols, 2009). The surrounding mudstone is deposited from suspension during the periods between storm events (Bowman & Johnson, 2013). The conglomerate that evolves upwards into sandstone beds with HCS may represent the storm waning and the associated reduction in grain size (Nichols, 2009).

The prevalence of the fair-weather signature (e.g., current ripples and parallel lamination) over the storm signature (e.g., HCS and SCS)

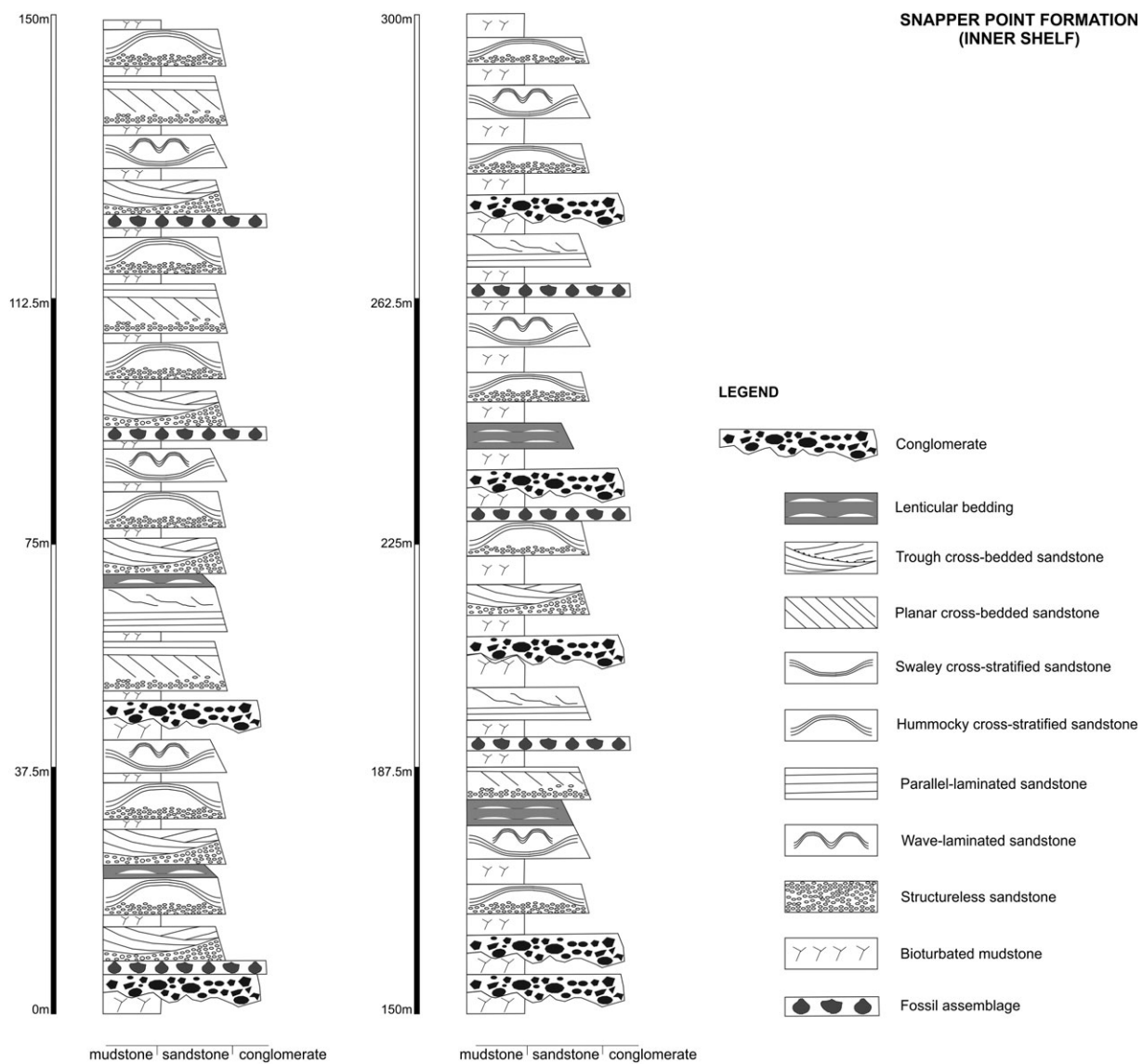


**FIGURE 14** Representative section of the Snapper Point Formation illustrating the sedimentological features of the inner shelf deposits. Note the upward increase in the frequency of individual storm-related events (tempestites)

indicates moderate storm influence, and this distribution of structures occurs in conjunction with tidally generated structures. This depositional environment exhibits an interbedding of both wave-generated structures and unidirectional structures, consistent to a tidally modulated lower shoreface (*sensu* Dashtgard et al., 2009; Dashtgard et al., 2012). The occurrence of glendonites is indicative of cold sea-floor environment (Thomas et al., 2007). The prevalence of distal *Cruziana* ichnofacies indicates abundance of permanent to semi-permanent dwellings of deposit-feeding organisms. This can be ascribed to cycles of higher energy and sediment winnowing related to shallower water conditions during low tide (Dashtgard et al., 2009). Their intercalation with *Skolithos* ichnofacies is in agreement with this generally higher energy condition.

## 4.5 | FA5: inner shelf (SPF)

### 4.5.1 | Description

This sedimentary succession is represented by a 300–400 m-thick succession and consists of extensive sheets of very fine- to very coarse-grained sandstone interbedded with mudstone layers (Figures 14 and

15a). The sandstone and mudstone beds are thin- to very thick-bedded (0.1–3 m). In places, the sandstone and mudstone form heterolithic bedding (F9), and some conglomeratic (F1) beds are also present. Sandstone is commonly trough (F3) and tabular cross-bedded (F5) (Figure 15b). Finer-grained sandstone is often planar parallel-laminated (F7) and can also contain HCS (F8). Sandstone with HCS contains hummocks that range in size from a few centimetres high and across to tens of centimetres high and across. Internally, the stratification of these hummocks is convex upwards and dips in all directions at angles of 10° or 20° (Figure 15c). Conglomerate is observed either at the bottom of coarse-grained sandstone beds or in the form of thin- to medium-bedded units (0.1–0.3 m), separated by mudstone beds (Figure 15d). They display sharp and/or erosive bases with the underlying mudstone and may be overlain by finer-grained sandstone with SCS or HCS. Loading features at the sandstone–mudstone interface are common, both load casts and ball and pillow structures. Bioturbation is intense even in sandstone beds leading to sediment agitation and homogenization into apparently structureless masses (Figure 15e). Intact shells are also preserved (Figure 15f).

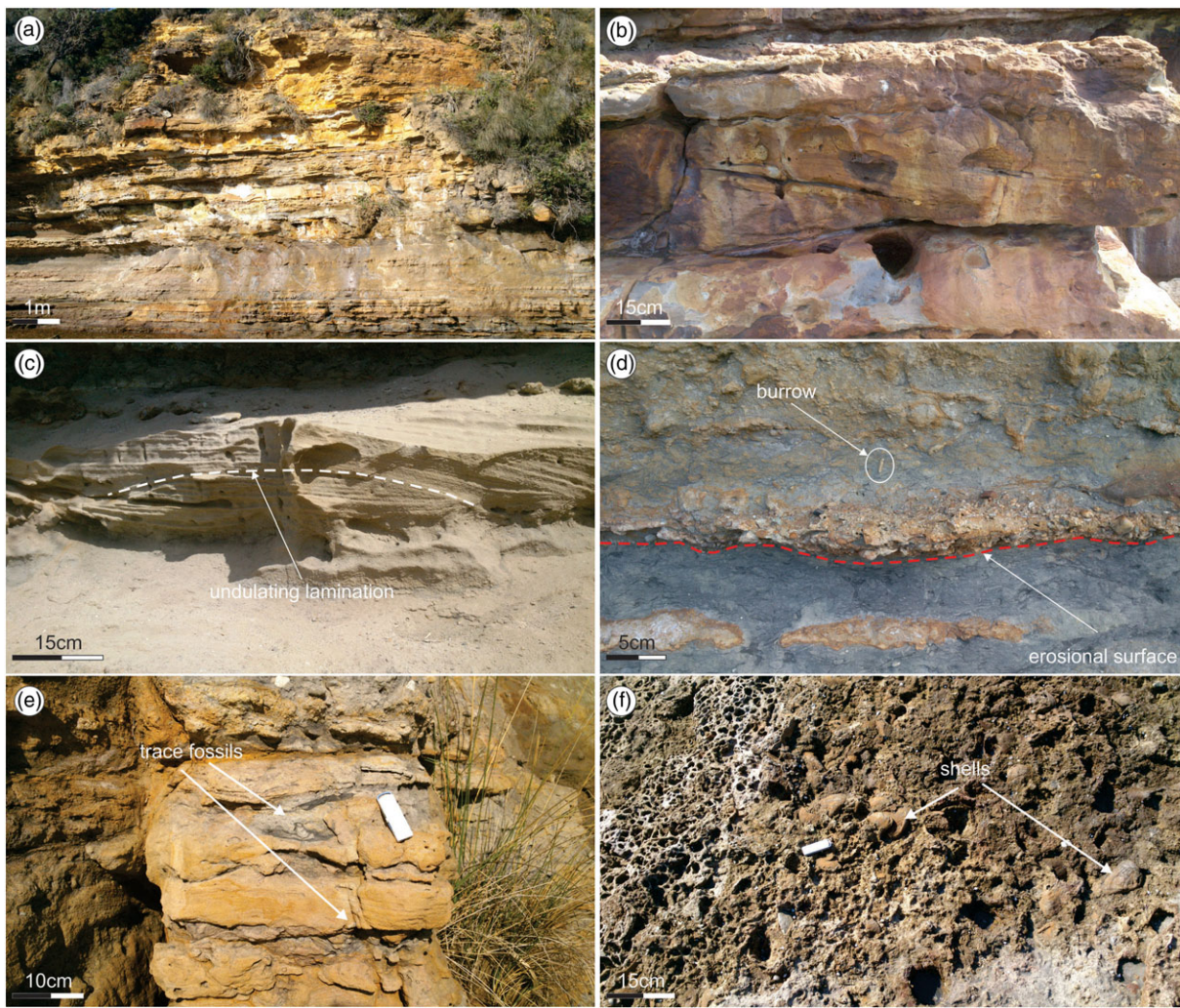


**FIGURE 15** Outcrop photographs from the inner shelf sediments in the southern Sydney Basin. (a) Thin- to thick-bedded sandstone interbedded with mudstone (Pretty Beach). (b) Tabular cross-stratified sandstone (Pretty Beach). (c) Hummocky cross-stratification-dominated sandstone (Bawley Point north). (d) Storm-associated conglomerate interbedded with mudstone (tempestite, Bawley Point north). (e) Fine-grained, bioturbated sandstone (Pretty Beach). (f) Condensed shell concentrations with some of the shells preserved in living or near living position (Clear Point) [Colour figure can be viewed at [wileyonlinelibrary.com](http://wileyonlinelibrary.com)]

#### 4.5.2 | Interpretation

These deposits are interpreted as inner shelf. The cross-bedding and cross-lamination are interpreted as the product of migration of subaqueous dunes. The planar erosion surfaces bounding the cross-beds are formed by the migration of the erosional trough in the lee of the migrating dunes (Reynaud et al., 2013). Heterolithic bedding indicates a tidally influenced depositional environment, and the SCS and HCS cross-stratification is interpreted to reflect combined flow action of both waves and storm-currents (Dumas & Arnott, 2006). The individual conglomeratic beds within the mudstone beds are also interpreted as storm-related deposits. Their sharp, possibly erosive base and gravel fill suggests that the scouring and initial deposition occurred when the storm was at its peak strength (Walker & Plint, 1992). Sediment load structures are indicative of sediment liquefaction that could have been triggered by pore-pressure changes associated with rapid burial and storm-related wave action (Lowe, 1976).

#### 4.6 | FA6: outer shelf (WS)

##### 4.6.1 | Description

This sedimentary succession is preserved as laterally extensive blanket-type deposits and is approximately 100 m thick (Figure 16). It is composed of fossiliferous mudstone and thin- to thick-bedded (0.1–0.8 m) sandstone forming thick (metres-scale) mudstone- and sandstone-dominated units (Figure 17a). Mudstone beds are greenish-brown, structureless (F10) to faintly laminated (F11), and moderately to intensely bioturbated. Fractured and intact shell fragments and thin-shelled bivalve debris are also observed, and some of them develop thin (centimetre-scale) accumulations (Figure 17b). Bioturbation is common in sandstone beds that may be enriched in fossils (Figure 17b). Trace fossils such as, *Skolithos*, *Cruziana*, and *Planolites* are abundant (Figure 17c). Sandstone beds are often structureless and locally amalgamated. Thin- to thick-bedded (0.1–0.5 m) sandstone, with local HCS (F8) and wave-modified current ripples

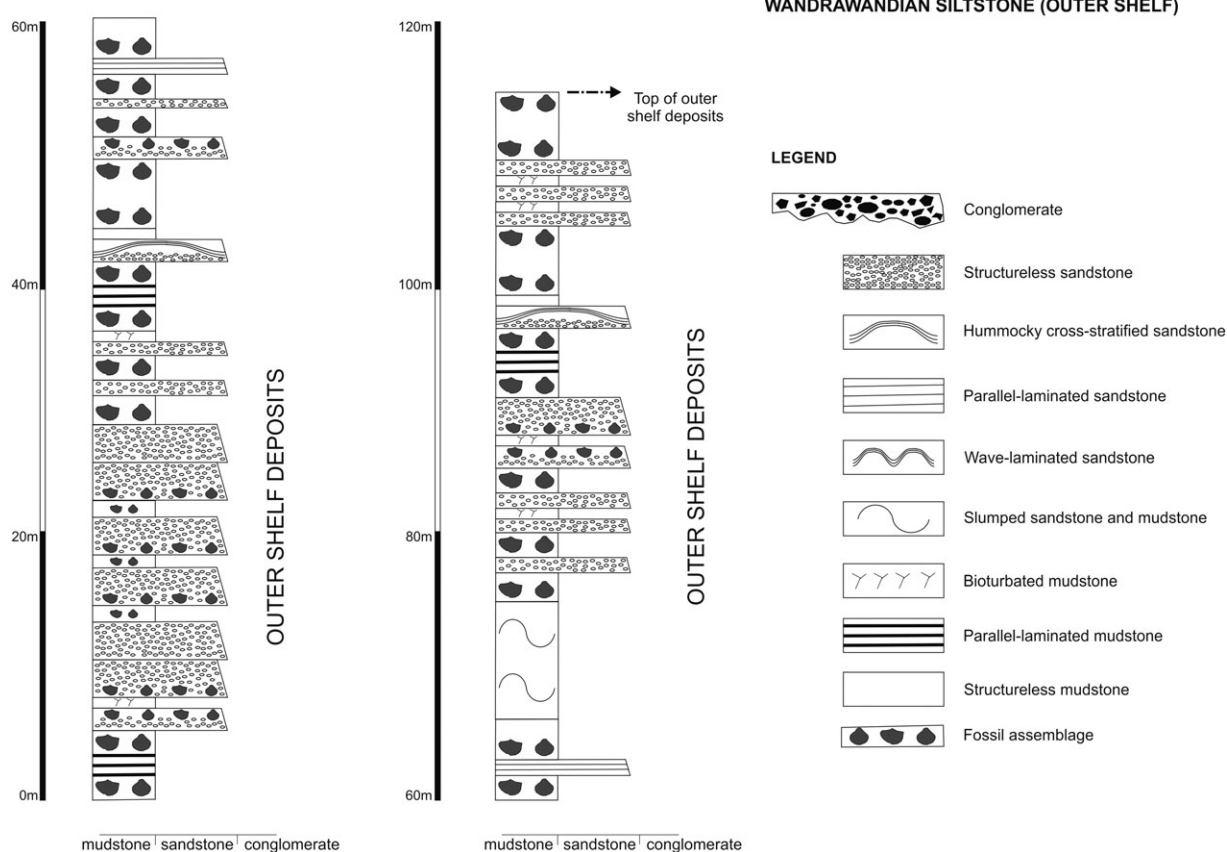


**FIGURE 16** Representative section of the Wandrawandian Siltstone presenting the sedimentological and biogenic features of the outer shelf deposits

(F6) occurs (Figure 17d). Thin- to medium-bedded (0.1–0.3 m) and normally graded sandstone beds are rare, whereas thin- to thick-bedded (0.1–0.5 m) sandstone with lensoidal geometry occurs (Figure 17e). These lensoidal beds may have erosional bases and common sole marks that include flute and gutter casts. Thick (up to 7 m) slumped units are present and contain recumbent soft-sediment folds and load balls (Figure 17f). Glendonites are abundant in WS and occur in discrete stratigraphic horizons, whereas the glendonite morphologies that are present are bladed, stellate and rosette forms.

#### 4.6.2 | Interpretation

These sedimentary strata are interpreted as outer shelf. The mudstone-dominated and laminated character of this depositional environment indicates accumulation mainly from suspension fallout in an outer shelf, fully marine environment. This is further supported by the trace-fossil assemblages that contain species that belong to the Zoophycos ichnofacies (Thomas et al., 2007). The occurrence of species such as Zoophycos, Chondrites, Planolites, Phycosiphon, Helminthopsis, and Cosmorhaphe is in agreement with an outer shelf environment of deposition. Shell accumulations in mudstone beds represent a community structure suited to an unstable softground substrate. The fossil-rich sandstone implies either a reduced rate of accumulation or a slightly more hospitable (sandy) substrate for shelled macrofauna (Abbott, 2000). The thin shell accumulations are interpreted as condensed sections. Preservation of parallel lamination in mudstone indicates suppression of bioturbating organisms, including shelled macrofauna.

This can be related to either anoxic conditions and scarce benthonic organisms or high sedimentation rates and turbidity, combined with a very fine-grained (inhospitable) substrate (Reading & Collinson, 1996). The low oxygenation levels can be also envisaged by the presence of Chondrites, which is commonly associated to tracemakers that are well adapted to very low-oxygen environments (Bromley, 1996), and often associated with organic-rich sediments.

Based on cumulative probability distributions of wave encounter (Peters & Loss, 2012), it has been highlighted that the sedimentary structures need to be utilized with caution when estimating the water depth (e.g., fair-weather vs. storm wave-base). It has been questioned that there is any correlation between the depth at which mean wave base intersects the seafloor and the storm-related events, which may reach the deeper water depths (outer shelf, below storm wave-base). The sandstone beds with HCS are interpreted as deposits from storm waves and/or relaxing storm surges. The sandstone beds with both HCS and wave-modified ripples are considered here as deposits accumulated in the outer shelf during storms and have been reworked into normal wave ripples by large fair-weather waves characterized by oscillatory flow, such as distantly generated storm swell. Thin-bedded, normally graded sandstone beds are interpreted as the result of deposition from distal storm-generated flows that alternate with mudstone deposited from suspension during fair weather. Thin-bedded mudstone and sandstone couples are interpreted as recording episodic influxes of mud and sand as river-fed hyperpycnites (Pattison, Ainsworth, & Hoffman, 2007) and/or storm-supported

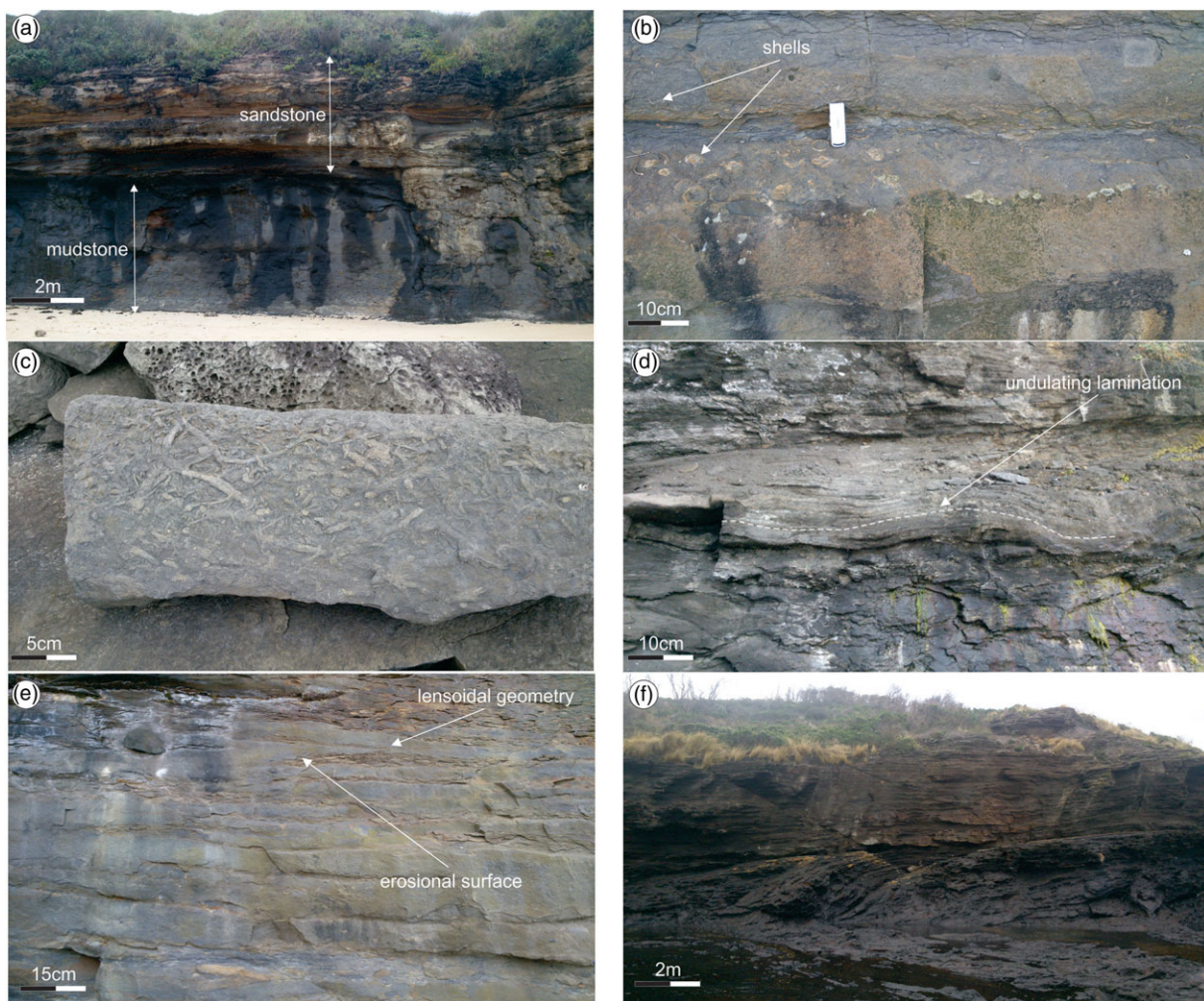


**FIGURE 17** Characteristic features of outer shelf deposits in the southern Sydney Basin (Dolphin Point). (a) Thick mudstone-dominated units separated by sandy intervals. (b) Shell-rich sandstone and mudstone bed. (c) Trace fossils seen at the base of the sandstone beds. (d) Sandstone bed with undulating lamination that reflects deposition from distal storm-generated flows. (e) Lensoidal sand body. (f) Large-scale deformation structure in the Wandrawandian Siltstone [Colour figure can be viewed at [wileyonlinelibrary.com](http://wileyonlinelibrary.com)]

gravity flows (Friedrichs & Wright, 2004; Hampson, 2010). The cause of the slumping remains controversial with possible mechanisms including abrupt rise of relative sea-level, increased rates of sedimentation, and seismicity (Thomas et al., 2007). The occurrence of glendonites is in agreement with glacier action during deposition of the WS and indicate bottom-water temperatures that were, at least seasonally, near-freezing (Fielding et al., 2006; Thomas et al., 2007).

## 5 | SEQUENCE STRATIGRAPHY

### 5.1 | Sequence stratigraphic surfaces, facies contacts, and shell concentrations

Sequence stratigraphic techniques and definitions have been the subject of numerous scientific papers (e.g., Cattaneo & Steel, 2003; Catuneanu, 2006; Catuneanu et al., 2009, 2011; Di Celma, Ragaini, Cantalamessa, & Landini, 2005; Dominguez & Wanless, 1991; Fielding et al., 2006; Helland-Hansen & Martinsen, 1996; Kidwell, 1991; Maravelis, Makrodimitras, Pasadakis, & Zelilidis, 2014; Milana

& Tietze, 2007; Plint & Nummedal, 2000; Posamentier & Allen, 1999; Sloss, Krumbein, & Dapples, 1949; Swenson & Muto, 2007). Surfaces that can serve, at least in part, as systems tract boundaries, are surfaces of sequence stratigraphic significance (Catuneanu, 2006). Facies contacts correspond to bounding surfaces of bedsets that are unrelated to changes in stratal stacking pattern (Catuneanu & Zecchin, 2013). They form within systems tracts, are generally diachronous surfaces, easily identified in the field, and can add constraints into the internal architecture of systems tracts (Zecchin & Catuneanu, 2013).

In the SSB, seven sequence stratigraphic surfaces and facies contacts were identified: (a) The subaerial unconformity (SU) that is designated by a nonconformity, and it is characterized by channelized truncations of the underlying basement by fluvial erosion (Figure 18a). This surface juxtaposes the underlying meta-sedimentary rocks from the overlying fluvial facies. (b) The maximum regressive surface (MRS), which is preserved as a conformable surface that separates the underlying lowstand fluvial sediments from the overlying transgressive bay-head delta facies. It is placed at the base of the earliest tidally influenced sediment, and it corresponds to the boundary between the WHF and PBF (Figure 18b). (c) The tidal-ravinement surface is placed

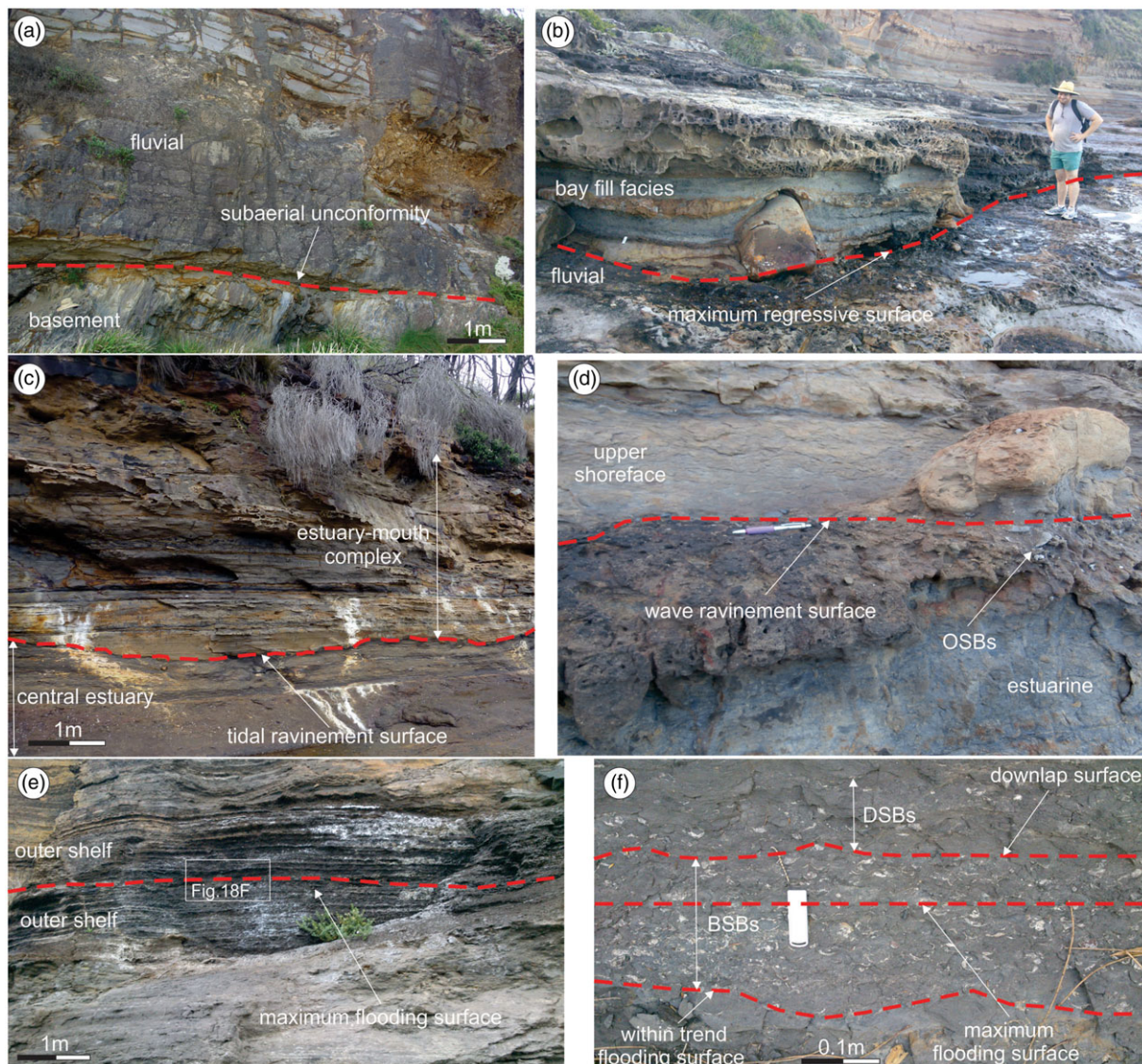


**FIGURE 18** Outcrop photographs depicting the sequence stratigraphic surfaces in the southern Sydney Basin. (a) Subaerial unconformity (Myrtle Beach). (b) Maximum regressive surface (Wasp Head). (c) tidal ravinement surface (Pebbley Beach). (d) Wave ravinement surface (Pebbley Beach). (e) Maximum flooding surface (Dolphin Point). (f) Within-trend flooding surfaces, maximum flooding surface, and downlap surface (Dolphin Point). Person for scale is 180 cm tall, pen is 15 cm long. BSBs = backlap shell beds; DSBs = downlap shell beds; OSBs = onlap shell beds [Colour figure can be viewed at [wileyonlinelibrary.com](http://wileyonlinelibrary.com)]

at the contact between the muddy central estuarine facies and the overlying sand-rich deposits of the estuary-mouth complex (Figure 18c). (d) The wave-ravinement surface (WRS) separates the underlying estuarine sediments from the overlying upper shoreface deposits. It is marked as a scour surface covered by condensed shell beds (condensed section) that are composed of intra-basinal skeletal material and concentrate on top of the WRS in the SSB (Figures 12e and 18d). These shells are interpreted as the onlap shell beds that have been deposited during transgression and mark the base of the marine transgressive deposits (Di Celma et al., 2005; Kidwell, 1991; Zecchin & Catuneanu, 2013). The WRS is associated with a firmground composed of sharp-walled and unlined burrows (Figure 18d). Firmground traces are dominated by vertical cylindrical-, U-, and subvertical-dwelling structures. (e) The maximum flooding surface (MFS) is placed within the outer shelf sediments, and it is represented by a condensed section (the backlap shell beds [BSBs]). BSBs are developed as a result of sediment starvation

and condensation (Kidwell, 1991; Zecchin & Catuneanu, 2013). The MFS is positioned at the heart of the BSBs, representing the time of maximum transgression (Figure 18e and 18f). (f) The downlap surface is placed within the outer shelf deposits, at the top of the BSBs (Figure 18f), and it is overlain by another condensed section (the downlap shell beds; Figure 18f). Downlap shell beds are less condensed, compared to BSBs, and also concentrate because of sediment starvation (Kidwell, 1991). (g) Within-trend flooding surfaces (WTFs) are developed at several different stratigraphic levels: at the contacts between upper shoreface and overlying lower shoreface; between lower shoreface and overlying inner shelf; and within the outer shelf facies (Figures 18f, 19a, and 19b). In some cases, the WTFs are related to condensed shell accumulations (Figure 19c), with some of them corresponding to the BSBs (Figure 18f) that develop close to the end of transgression (Di Celma et al., 2005). The BSBs are 15 cm thick and preserve faunas in life or near life position.

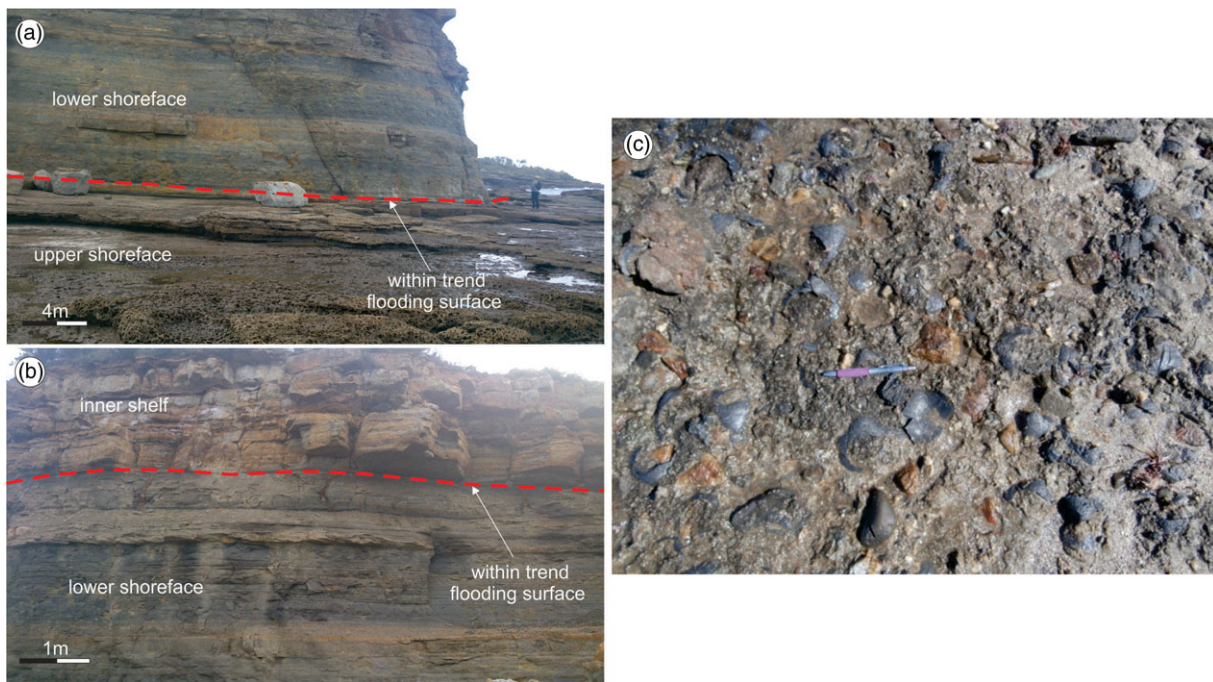


**FIGURE 19** Outcrop examples of the within-trend flooding surfaces and related shell concentrations in the southern Sydney Basin. (a) Upper shoreface/lower shoreface boundary (Pebbly Beach). (b) Lower shoreface/inner shelf boundary (Clear Point). (c) Shell bed at the top of (b) (Clear Point). Pen for scale is 15 cm long [Colour figure can be viewed at [wileyonlinelibrary.com](http://wileyonlinelibrary.com)]

## 5.2 | Sequence stratigraphic interpretations

Three systems tracts are interpreted in the SSB: lowstand (LST), transgressive (TST), and highstand (HST) (Figures 20 and 21). A correlation of selected stratigraphic logs, highlighting sequence stratigraphic surfaces and geometries of the depositional systems and systems tracts is illustrated in Figure 22.

The LST consists of progradational deposits that form during the early stages of relative sea-level rise, when the rates of sediment supply outpace those of accommodation creation (Catuneanu, 2002, 2006; Posamentier & Allen, 1999). Underlying the LST, the SU forms during forced regression, and its areal extent depends on the magnitude of relative fall and the topographic gradients of the subaerially exposed surface (Catuneanu, 2006; Ethridge, Germanoski, Schumm, & Wood, 2001). In the SSB, the LST is represented by the fluvial facies that overlie the basement rocks along the SU (Figures 20–22). The erosional character of the SU indicates reworking by the high-energy fluvial system, which is interpreted as braided rivers associated with relatively steep topographic gradients. The fluvial section displays an overall fining-upward trend and an up-sequence increase in the ratio between floodplain and channel deposits. These characteristics suggest an increase with time in the rate of creation of accommodation, in parallel with a progressive decrease in energy as a result of coastal upstepping and the associated lowering of topographic gradients in the fluvial system (Catuneanu, 2006). The top of the LST is marked by the MRS, whose timing corresponds to the end of progradation. In the SSB, the MRS is generally preserved with the exception of areas affected by subsequent transgressive wave-ravinement erosion.

The TST is composed of retrogradational deposits developed during relative sea-level rise, when the rates of accommodation creation outpace those of sedimentation at the shoreline (Catuneanu, 2002;

Posamentier & Allen, 1999). In the SSB, the TST includes the estuarine system, the upper and lower shoreface, the inner shelf, and the lower part of the outer shelf sediments. It is bounded by the MRS at the base and by the MFS at the top (Figures 20–22). Within the study area, the top of the estuarine system is marked by the WRS (Figures 20–22). In the SSB, the transgressive facies are thick and, for most part, the WRS does not rework the MRS and the SU. These characteristics suggest high rates of coastal aggradation and relatively low rates of transgression. The WRS is overlain by onlap shell beds that reflect the result of low net deposition due to sediment bypass (Kidwell, 1991). The occurrence of several WTSs within the TST is indicative of episodic subsidence and, therefore tectonic activity, in the SSB.

The HST consists of progradational deposits that form when sediment accumulation rates exceed the rate of increase in accommodation during the late stages of relative sea-level rise (Catuneanu, 2003, 2006). In the SSB, the HST bottomset corresponds to the upper part of the outer shelf deposits that overlay the MFS (Figures 20–22). The BSBs are associated with the MFS and indicate interaction of major storm waves and shelf currents, while the life or near life position of the shells suggest a relatively low-energy environment. The condensed sections separated by the downlap surface and MFS indicate low sediment input and variable degree of erosion (Di Celma et al., 2005; Kidwell, 1991; Zecchin & Catuneanu, 2013).

## 6 | DISCUSSION

### 6.1 | Marine versus fluvial origin of the WHF

The precise depositional environment of the WHF has been debated (Cisterna & Shi, 2014; Eyles et al., 1998; Fielding et al., 2006;

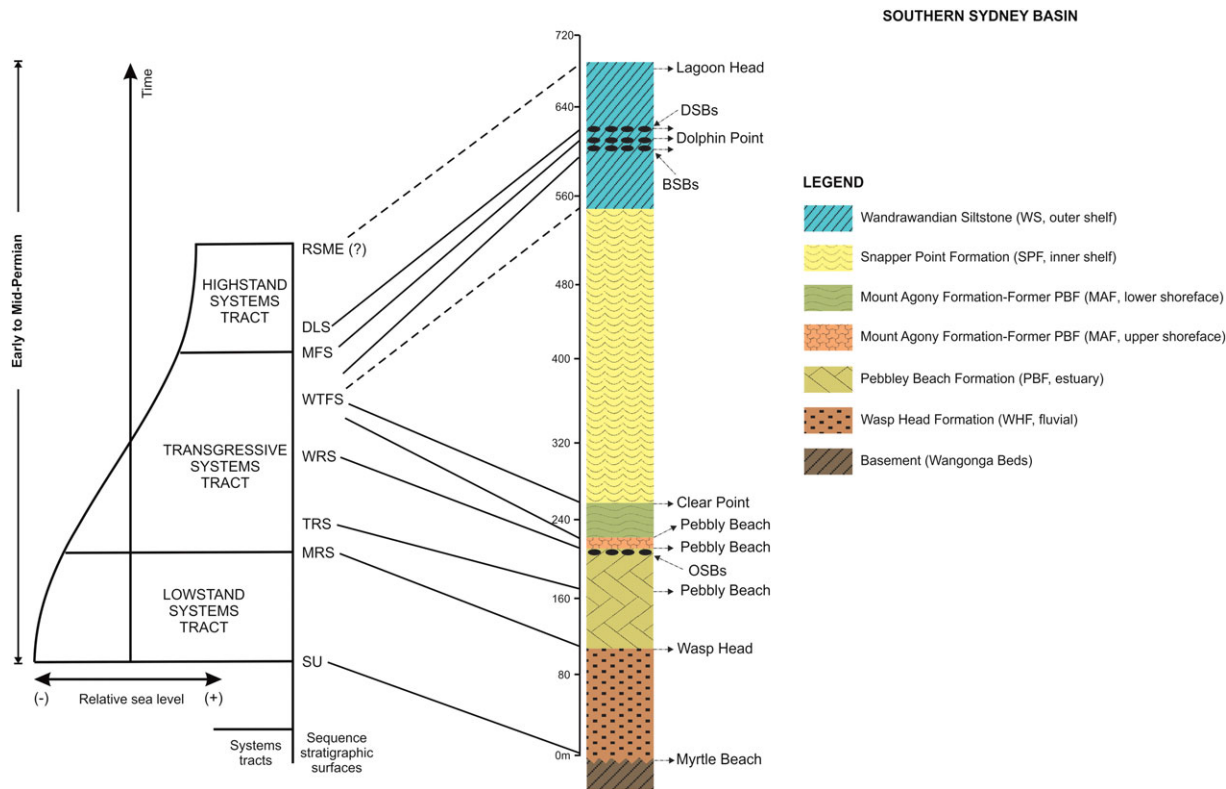


**FIGURE 20** Sequence stratigraphic framework for the southern Sydney Basin. Note the (1) long-term (second-order) deepening-upward trend from fluvial facies to outer shelf deposits and the following shoaling-upward trend towards the shoreface deposits; (2) interpretation of the depositional facies in terms of third-order systems tracts. Dashed lines represent inferred sequence stratigraphic surfaces. BSBs = backlap shell beds; DLS = downlap surface; DSBs = downlap shell beds; MFS = maximum flooding surface; MRS = maximum regressive surface; OSBs = onlap shell beds; RSME = regressive surface of marine erosion; SU = subaerial unconformity; TRS = tidal ravinement surface; WRS = wave ravinement surface; WTFS = within-trend flooding surface [Colour figure can be viewed at [wileyonlinelibrary.com](http://wileyonlinelibrary.com)]

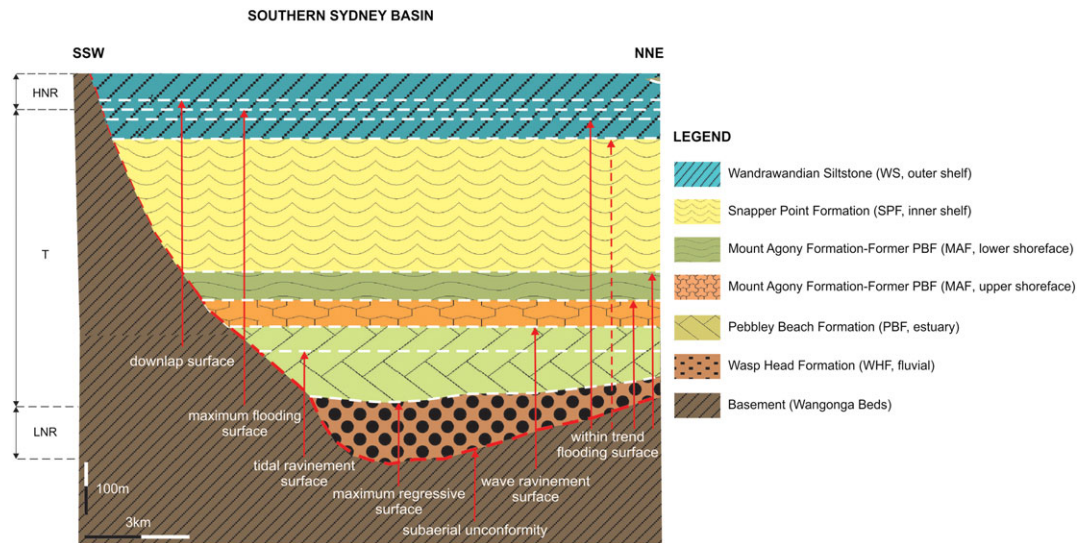


**FIGURE 21** Schematic vertical cross-section of the southern Sydney Basin composed of a tide-dominated estuary that is situated in an unincised valley. The succession initially deepens upwards, with fluvial sediments that are overlain by bay-head delta facies that prograde in an estuarine, capped by shelf deposits and, eventually shoals with deposition of shoreface deposits. Note the position of sequence stratigraphic sequences and the subdivision of the depositional sequence with respect to the shoreline trajectories. HNR = highstand normal regression; LNR = lowstand normal regression; NNE = north-north-east; SSW = south-southwest; T = transgression [Colour figure can be viewed at [wileyonlinelibrary.com](http://wileyonlinelibrary.com)]

Rygel et al., 2008a; Thomas et al., 2007; Tye et al., 1996), but an overall marine nature has been generally accepted. The principal lines of evidence include the occurrence of (a) subaqueous debris-flow breccias;

(b) enormous exotic clasts that must have been dropped from floating ice through a water column; (c) occurrence of HCS and SCS; (d) a widespread though restricted suite of marine trace fossils; and (e) a rich

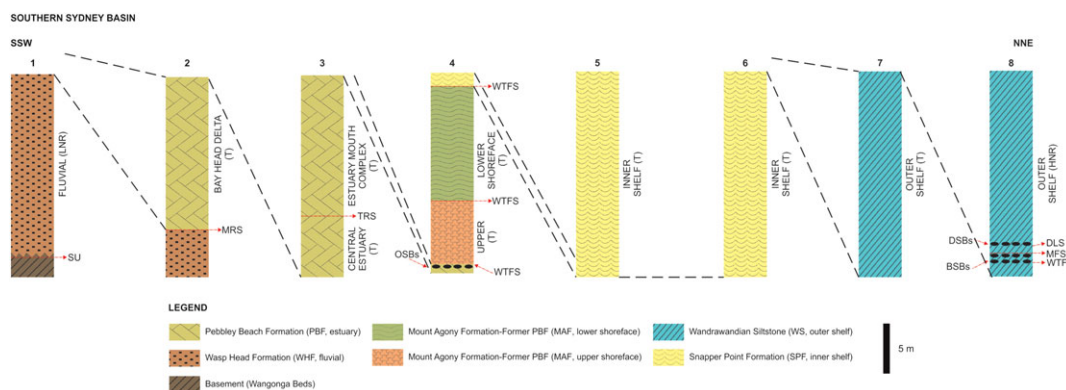


**FIGURE 22** Cross-section of selected stratigraphic logs that illustrates the proposed sequence stratigraphic framework for the southern Sydney Basin. DLS = downlap surface; HNR = highstand normal regression; LNR = lowstand normal regression; MFS = maximum flooding surface; MRS = maximum regressive surface; NNE = north-north-east; SSW = south-southwest; SU = subaerial unconformity; T = transgression; TRS = tidal ravinement surface; WRS = wave ravinement surface; WTFS = within-trend flooding surface [Colour figure can be viewed at [wileyonlinelibrary.com](http://wileyonlinelibrary.com)]

assemblage of marine body fossils including the cold-climate marine bivalve *Eurydesma*. In particular, three main fossil accumulations have been documented (Cisterna & Shi, 2014). The lower and middle assemblages are bivalve-dominated and contain scarce brachiopods, in contrast to the uppermost that is brachiopod-dominated.

The present investigation proposes a fluvial origin for the WHF and revises the formation boundary between the WHF and the overlying PBF to a lower stratigraphic level (Figures 18b, 20, 21, and 22). In sequence stratigraphic terms, the new formation boundary corresponds to the MRS at the limit between sand-rich fluvial and mudstone-dominated bay-head delta deposits. This lithostratigraphic revision reassigns the upper (marine) portion of the former WHF to the lower part of the PBF. The revised stratigraphic section (formerly assigned to the WHF, and now to the lowermost part of the PBF) is also reinterpreted here as bay-fill and bay-head delta deposits (Figures 7, 9, and 18b). The fluvial origin of the newly defined WHF is supported by as follows: (a) The evidence of transport at the basal shear zone (bullet-shaped clasts) and the clast imbrication in the breccias. (b) In addition to the marine realm, diamictites also develop through sediment gravity flows, lodgement, deformation, and bulldozing at the ice margin (Arnaud & Etienne, 2011). In such settings, the clasts include evidence of recent transport in the basal traction zone including faceting, striations, chattermarks and bullet-shape. Bullet-shaped clasts and clast imbrication are well developed in the studied diamictites (Figure 5d and 5e). These enormous clasts display well-developed stoss and lee sides, and the units exhibit a strong  $\alpha$ -axis fabric, indicating flow transportation. They also portray evidence of ploughing and lodgement (prows), meeting many of the characteristics of a lodgment and deformation tillite associated with a glacially influenced fluviolacustrine depositional setting. (c) This study did not record any HCS or SCS in the observed sections. Only scarce examples of HCS and SCS have been reported in previous publications; some are associated with coarse-grained sediment (very coarse-grained sandstone and conglomerate), and they lack characteristic undulating laminae (Figures 7c and 9c in Rygel et al., 2008a). These observations do not fit with the sedimentological characteristics of the HCS and SCS. Others are located above the MRS, in a marine setting, which is in agreement with the environment of occurrence of HCS and SCS

(Figures 10b and 10c in Rygel et al., 2008a), as well as with our own observations. (d) The marine trace fossils assemblages are only found above the MRS (Emily Miller Beach and the lower 5 m of the Durras North section in Rygel et al., 2008a). The interpretation of this part of the stratigraphic section as bay-fill and bay-head delta deposits also justifies the occurrence of marine trace fossils (e.g., *Diplocraterion habichi*, *Taenidium* isp, and *Phycosiphon*). (e) No brachiopods have been recorded by this investigation in the lower and middle bivalve-dominated assemblages of Cisterna and Shi (2014). The lack of evidence of resistance to predation in the bivalves also supports their fluvial origin (Figures 5f and 6a). The upper brachiopod-dominated assemblage (with *Eurydesma*) is located above the MRS, in a marine-influenced depositional environment (bay-fill and bay-head; Figure 18b) and is consistent with the recorded palaeoecology of Rygel et al. (2008a).

These observations suggest a shift in the depositional environments across the MRS. The underlying facies record transport along the basal shear zone and make the glacially influenced fluvial setting and associated glacio-lacustrine facies as the most plausible interpretation for the WHF. Additional evidence comes from the presence of (a) floating pebbles and their horizontal stratification in the sandstone beds; (b) abundance of large-scale trough cross-bedding; (c) alternating foresets of sandstone and conglomerate within the cross-bedded sets; and (d) downstream accreting barform deposits, which are typical of braided-fluvial systems. Furthermore, the generally coarse-grained nature of the sand deposits, in conjunction with the scarcity of mudstone and the common presence of planar cross-bedding, has long been ascribed to braided fluvial systems (Bristow, 1988; Medici et al., 2015). The overlying facies (lowermost part of the PBF here) do document marine influence and are consistent with a prograding bay-head delta.

## 6.2 | Uppermost PBF (Mt. Agony Formation): a tidally modulated shoreface?

There is a general consensus that the PBF encompasses a broad range of depositional environments and sub-environments that include marginal- and shallow-marine settings (e.g., Bann, Fielding,

MacEachern, & Tye, 2004; Fielding et al., 2006; Gostin & Herbert, 1973; Tye et al., 1996). The integrated sedimentologic and sequence stratigraphic analysis presented here indicates that the PBF includes lithologically distinct units that belong to both marginal-marine (bay-head delta, central estuary, and estuary-mouth complex, the lower part) and shallow-marine (upper and lower shoreface, the upper part). It is therefore suggested that the shallow-marine part of the PBF may be better regarded as the new Mt. Agony Formation (MAF, new proposed name). The new formation boundary, as defined based on sedimentological and sequence stratigraphic criteria, is represented by the WRS and is positioned at the limit between the estuary-mouth complex deposits and the overlying upper shoreface sediments. This consideration redesignates the uppermost (shallow-marine) part of the former PBF to the MAF. The uppermost stratigraphic section (previously considered as the PBF, and now as MAF) is represented by upper and lower shoreface deposits (Figures 11–13, and 18d).

Tidally modulated shorefaces (TMSs) occur in modern macrotidal to megatidal settings (Dashtgard et al., 2009). These settings are affected by strong wave energies and by strong tides, with the latter facilitating the lateral migration of wave zones along the depositional profile of the beach and shoreface (Dashtgard et al., 2009; Dashtgard et al., 2012). Despite their common occurrence in the modern environments (e.g., Anthony, Levoy, Monfort, & Degryse-Kulkarni, 2005; Levoy, Monfort, & Larsonneur, 2001), our knowledge about the impact of tides on the shoreface relies on few modern and ancient examples (Dashtgard & Gingras, 2007; Dashtgard, Gingras, & Butler, 2006; Frey & Dashtgard, 2012), and the available criteria for the recognition of TMS are restricted to a single modern (Dashtgard et al., 2009) and a single ancient example (Ainsworth et al., 2008). The research of Ainsworth et al. (2008) and Dashtgard et al. (2009) provides insights in the sedimentological and ichnological character of prograding TMS, and the diagnostic criteria, as summarized by Dashtgard et al. (2012), include (a) interbedding of sedimentary structures down the shoreface profile; (b) absence of a well-defined middle shoreface; (c) presence of an anomalously thick foreshore; (d) presence of trace-fossil suites comprising structures common to both the *Skolithos* and *Cruziana* ichnofacies in lower shoreface units.

With respect to the above-mentioned criteria, the MAF displays similar: (a) intercalation of oscillatory and combined-flow structures; (b) lack of units that include the standard sedimentological and ichnological diagnostic features of the middle shoreface (e.g., swaley cross-stratification and trace fossils of the archetypal *Skolithos* ichnofacies). A similar feature has been described by Dashtgard et al. (2009) and has been attributed to the lateral translation of wave zones across the TMS; and (c) *Skolithos* and *Cruziana* ichnofacies in the lower shoreface. Furthermore, the retrograding MAF exhibits a similar increase in the mud:sand ratio, similar to the TMS described by Ainsworth et al. (2008). It also includes features that are similar to those recorded in tidally influenced settings, such as the increase in the grain size of the sand from the upper to the lower shoreface, which is a common trend in such settings (Frey & Dashtgard, 2012).

In contrast to the prograding TMS, the studied shoreface lacks of the diagnostic decrease in both the diversity of ichnogenera and the

density of burrowing across the shoreface profile. The study of Fielding et al. (2006) offers a systematic ichnological approach and revealed the occurrence of heavily bioturbated strata in the lower shoreface and an associated up-sequence increase in the degree of bioturbation. This trend can be associated to the overall transgressive nature the MAF, as indicated by the presence of more marine trace fossil assemblages across the shoreface profile and the sequence stratigraphic analysis. This increase in the density of burrowing can be also associated with physicochemical stresses acting upon the depositional environment (Mackay & Dalrymple, 2005). Fluvial systems influence the sedimentological-ichnological characteristics of prograding shorefaces (Ainsworth, Vakarelov, & Nanson, 2012). The input of fluvial derived material results in an increase in the volume of sand and mud to the shoreline and is coupled with elevated water turbidities and salinity variations (Dashtgard et al., 2012). The depositional environment and the lithologic composition of the TMS described by Ainsworth et al. (2008) and the MAF are similar, but exhibit strikingly different degrees of bioturbation. The high density of trace fossils in the studied lower shoreface can be ascribed to the limited fluvial influence and the associated lower sedimentation rates and limited fresh water input.

The presented example indicates that the common intercalation of sedimentary structures across the shoreface profile and the lack of a well-defined middle shoreface are common features in TMS irrespective of the involved shoreline trajectory. The different degree of bioturbation between the prograding TMS and the studied retrograding TMS highlights the need for further research towards the better understanding of the impact of environmental conditions, fluvial input, and shoreline trajectory on sedimentation processes in shallow-marine settings.

### 6.3 | Allocyclic controls on sequence development

Pre-Cenozoic icehouse periods are not well-understood, mainly because of the general lack of precise geochronological data and thus, their character is still controversial. During the mid-Carboniferous to Early Permian, discrete glacial periods separated by warmer periods have been documented in eastern Australia (Eyles et al., 1998; Fielding et al., 2006; Isbell, Miller, Wolfe, & Lenaker, 2003; Jones & Fielding, 2004; Tye et al., 1996). Supporting evidence also comes from northeast Australia (Queensland; Figure 1a), where three icehouse periods have been documented (Jones & Fielding, 2004). Diamictites in the WHF are associated with the melting of glaciers. As an analogue, Pleistocene outwash rivers and fluviolacustrine settings with diamictites have been reported in the western Scottish Highlands (Golledge, 2007) and the southeastern Alps (Tagliamento River; Monegato & Stefani, 2010). Glendonites are abundant in the studied succession (MAF and WS) and indicate deposition under cold climatic conditions that have been related to the last period of Gondwanan glaciation (Fielding et al., 2006; Thomas et al., 2007). Glendonites in the upper part of the SSB (Broughton Formation and lower Illawarra Coal Measures; Figure 2) indicate continuous icehouse conditions during the mid- to Late Permian (Selleck, Carr, & Jones, 2007). Conodont apatite  $\delta^{18}\text{O}$  data also indicate that the main deglaciation would have occurred during this

time (Kungurian to Capitanian) (Chen et al., 2013). Other evidence for post-Early Permian (post-Sakmarian) glaciers has been reported from Western Australia (Fielding et al., 2008) and Siberia (Chumakov, 1994) until the late Capitanian.

Recently published studies indicate a decrease in the magnitude of the eustatic sea-level changes from up to 120 m (late Pennsylvanian to mid-Sakmarian) to 30–70 m (mid-Sakmarian) and 10–60 m (Roadian through Capitanian) (Rygel, Fielding, Frank, & Birgenheier, 2008b). These estimated eustatic sea-level changes are unable to account for the accumulation of 700 m of sediments in non-marine (fluvial) to outer shelf depositional environments, which is more consistent with tectonically driven subsidence. Orbitally driven glacio-eustatic sea-level fluctuations have been documented in other sedimentary basins, including the Crotone Basin, Italy (Zecchin, 2005) and the Wanganui Basin, New Zealand (Naish & Wilson, 2009). These basins display similar stratigraphic records that consist of thick cyclothem successions, with each cyclothem being thought as the result of a single orbitally driven glacio-eustatic sea-level cycle. However, such cyclic pattern is not observed in the sedimentary succession of the SSB.

The study of the broad-scale stratigraphic architecture in the SSB reveals an Early Permian general aggradational–retrogradational trend (WHF to lower WS), followed by an aggradational trend (upper WS). This architecture involves long-term trends in the formation of stacking patterns, with no development of glacio-eustatic cycles over shorter time scales. Thus, it is concluded that Early Permian sedimentation pattern in the SSB may reflect a major episode of tectonic subsidence along the Australian continental margin, with rates high enough to suppress the effects of higher frequency eustatic fluctuations, explaining the lack of high-frequency cyclothems in the stratigraphic record. Similar trends have been documented in the Borbón Basin, northwest Ecuador. The sedimentary succession in the Borbón Basin has been regarded as being accumulated along a narrow, active continental margin during tectonically induced transgression (Di Celma et al., 2010).

Therefore, it is inferred that the rates of regional tectonic subsidence in the SSB were higher than the rates of glacio-eustatic fall related to the higher frequency orbital cycles, thus sustaining a continuous rise in relative sea level. The rates of relative sea-level rise would have been enhanced during stages of glacio-eustatic rise, resulting in fast creation of accommodation and the consequent formation of the observed WTSs within the TST. Conversely, the rates of relative sea-level rise would have been lower during stages of glacio-eustatic fall. The thick transgressive deposits documented within the SSB indicate prolonged backstepping of the shoreline driven by long-term subsidence, as well as high subsidence rates outpacing both the rates of eustatic fall and the rates of sedimentation at the shoreline. This is consistent with an extensional, fault-bounded rift setting. It appears that the basin physiography played an important role in the stratigraphic architecture of SSB.

## 7 | CONCLUSIONS

The Lower Permian sedimentation in the SSB provides a case study for a depositional sequence developed during icehouse periods. This study

illustrates the sequence stratigraphic architecture that may develop under variable tectonic and eustatic conditions, and several conclusions regarding the effect of allocyclic factors on stratigraphic architecture can be drawn based on the observed stratigraphic features.

- The studied sequence accumulated in sedimentary basin that resembles a fault-bounded rift basin and encompasses a wide spectrum of depositional environments, ranging from non-marine (fluvial) to shallow-marine (outer shelf). They are arranged into a pattern that documents an initial regional deepening-upward trend (Upper Permian WHF, PBF, MAF, SPF, and WS).
- The stratigraphic architecture is arranged into systems tracts that make up an almost complete depositional sequence with an asymmetric architecture. Transgressive (PBF, MAF, SPF, and lower WS) deposits are thicker compared to the regressive section (WHF during lowstand normal regression and upper WS during highstand normal regression), as a consequence of the prolonged and fast subsidence that controlled deposition in this sedimentary basin during the transgressive phase.
- During the Early Permian time, enhanced tectonically driven subsidence controlled the basin-fill conditions, with eustatic sea-level fluctuations being suppressed. This rapid tectonically induced subsidence overpowered the inferred eustatic falls and promoted quick creation of accommodation during eustatic rises. The high sedimentation rates, in conjunction with the steep slope gradients, led to the deposition of thick transgressive deposits.

## ACKNOWLEDGEMENTS

This research was financially supported by the NSW Institute for Frontiers Geosciences (IFG), through the research project: Palaeogeographic and geotectonic evolution of the Myall Trough and Sydney Basin: Constraints in the Permian geological history of eastern Australia (Prof. W. J. Collins). This study was conducted by the (a) Laboratory of Sedimentology, Department of Geology, University of Patras, Greece; (b) Department of Earth and Atmospheric Sciences, University of Alberta, Canada; and (c) School of Environmental and Life Sciences, University of Newcastle, Australia. The authors wish to acknowledge the journal editor Shane Tyrrell, as well as the journal reviewers Massimo Zecchin and Jorge Magalhães for the constructive and valuable reviews that greatly improved the manuscript. Our colleague Jake Breckenridge is acknowledged for constructive discussions about the basin-fill conditions in the SSB.

## REFERENCES

- Abbott, S. T. (2000). Detached mud prism origin of highstand systems tracts from mid-Pleistocene sequences, Wanganui Basin, New Zealand. *Sedimentology*, 47, 15–29.
- Ainsworth, R. B., Flint, S. S., & Howell, J. (2008). Predicting coastal depositional style: Influence of basin morphology and accommodation/sediment supply regime within a sequence stratigraphic framework. In G. J. Hampson, R. J. Steel, P. B. Burgess, & R. W. Dalrymple (Eds.), *Recent advances in shallow-marine stratigraphy* (pp. 237–263). SEPM Special Publication 90.
- Ainsworth, R. B., Vakarelov, B. K., & Nanson, R. A. (2012). Dynamic spatial and temporal prediction of changes in depositional processes on clastic

- shorelines: Towards improved subsurface uncertainty reduction and management. *American Association of Petroleum Geologists Bulletin*, 95, 267–297.
- Allen, J. R. L. (1982). *Sedimentary structures: Their character and physical basis*. Amsterdam: Elsevier Scientific Publishing Company, 679 pp.
- Anthony, E. J., Levoy, F., Monfort, O., & Degryse-Kulkarni, C. (2005). Short-term intertidal bar mobility on a ridge-and-runnel beach, Merlimont, northern France. *Earth Surface Processes and Landforms*, 30, 81–93.
- Arnaud, E., & Etienne, J. L. (2011). Recognition of glacial influence in Neoproterozoic sedimentary successions. In E. Arnaud, G. P. Halverson, & G. Shields-Zhou (Eds.), *The geological record of Neoproterozoic glaciations* (Vol. 36) (pp. 39–50). Geological Society London Memoirs.
- Bann, K. L., Fielding, C. R., MacEachern, J. A., & Tye, S. C. (2004). Differentiation of estuarine and offshore marine deposits using integrated ichnology and sedimentology. In D. McIlroy (Ed.), *The application of ichnology to palaeoenvironmental and stratigraphic analysis* (Vol. 228) (pp. 179–211). Geological Society Special Publication.
- Dott, R. H. Jr., & Bourgeois, J. (1982). Hummocky stratification: Significance of its variable bedding sequences. *Geological Society of America Bulletin*, 93, 663–680.
- Bowman, P. A., & Johnson, D. H. (2013). Storm-dominated shelf-edge delta successions in a high accommodation setting: The palaeo-Orinoco Delta (Mayaro Formation), Columbus Basin, South-East Trinidad. *Sedimentology*, 61, 792–835.
- Bridge, J. S. (2003). *Rivers and floodplains: Forms, processes, and sedimentary record*. Oxford: Blackwell 504 pages.
- Bridge, J. S. (2006). Fluvial facies models: Recent developments. In W. Posamentier, & R. G. Walker (Eds.), *Facies models revisited* (Vol. 84) (pp. 85–170). SEPM Special Publication.
- Bristow, C. S. (1988). Controls on the sedimentation of the Rough Rock Group (Namurian) from the Pennine Basin of northern England. In B. M. Besly, & G. Kelling (Eds.), *Sedimentation in a synorogenic basin complex: The Upper Carboniferous of Northwest Europe* (pp. 114–131). Blackie Glasgow.
- Bromley, R. G. (1996). *Trace fossils: Biology, taphonomy, and applications* (2nd ed.). London: Chapman and Hall.
- Budillon, F., Vicinanza, D., Ferrante, V., & Iorio, M. (2006). Sediment transport and deposition during extreme sea storm events at the Salerno Bay (Tyrrhenian Sea): Comparison of field data with numerical model results. *Natural Hazards and Earth System Sciences*, 6, 839–852.
- Cantalamessa, G., & Di Celma, C. (2004). Sequence response to syndepositional regional uplift: Insights from high-resolution sequence stratigraphy of late Early Pleistocene strata, Periadriatic Basin, central Italy. *Sedimentary Geology*, 164, 283–309.
- Castelltort, S., Guillocheau, F., Robin, C., Rouby, D., Nalpas, T., Lafont, F., & Eschard, R. (2003). Fold control on the stratigraphic record: A quantified sequence stratigraphic study of the Pico del Aguila anticline in the south-western Pyrenees (Spain). *Basin Research*, 15, 527–551.
- Cattaneo, A., & Steel, R. J. (2003). Transgressive deposits: A review of their variability. *Earth-Science Reviews*, 62, 187–228.
- Catuneanu, O. (2002). Sequence stratigraphy of clastic systems: Concepts, merits, and pitfalls. *Journal of African Earth Sciences*, 35, 1–43.
- Catuneanu, O. (2003). Sequence stratigraphy of clastic systems. *Geological Association of Canada, Short Course Notes*, 16, 248.
- Catuneanu, O. (2004). Basement control on flexural profiles and the distribution of foreland facies: The Dwyka Group of the Karoo Basin, South Africa. *Geology*, 32, 517–520.
- Catuneanu, O. (2006). *Principles of sequence stratigraphy*. Amsterdam: Elsevier 386.
- Catuneanu, O., Abreu, V., Bhattacharya, J. P., Blum, M. D., Dalrymple, R. W., Eriksson, P. G., ... Winker, C. (2009). Towards the standardization of sequence stratigraphy. *Earth-Science Reviews*, 92, 1–33.
- Catuneanu, O., Galloway, W. E., Kendall, C. G. S. T. C., Miall, A. D., Posamentier, H. W., Strasser, A., & Tucker, M. E. (2011). Sequence stratigraphy: Methodology and nomenclature. *Newsletters on Stratigraphy*, 44, 173–245.
- Catuneanu, O., Hancox, P. J., Cairncross, B., & Rubidge, B. S. (2002). Foredeep submarine fans and forebulge deltas: Orogenic off-loading in the underfilled Karoo Basin. *Journal of African Earth Sciences*, 35, 489–502.
- Catuneanu, O., Khalifa, M. A., & Wanas, H. A. (2006). Sequence stratigraphy of the Lower Cenomanian Bahariya Formation, Bahariya Oasis, Western Desert, Egypt. *Sedimentary Geology*, 190, 121–137.
- Catuneanu, O., Martins-Neto, M., & Eriksson, P. G. (2005). Precambrian sequence stratigraphy. *Sedimentary Geology*, 176, 67–95.
- Catuneanu, O., Sweet, A. R., & Miall, A. D. (1999). Concept and styles of reciprocal stratigraphies: Western Canada foreland basin. *Terra Nova*, 11, 1–8.
- Catuneanu, O., & Zecchin, M. (2013). High-resolution sequence stratigraphy of clastic shelves II: Controls on sequence development. *Marine and Petroleum Geology*, 39, 26–38.
- Chen, B., Joachimski, M. M., Shen, S., Lambert, L. L., Lai, X., Wang, X., ... Yuan, D. (2013). Permian ice volume and palaeoclimate history: Oxygen isotope proxies revisited. *Gondwana Research*, 24, 77–89.
- Chumakov, N. M. (1994). Evidence of Late Permian glaciation in the Kolyma River Basin: A repercussion of the Gondwanan glaciations in Northeast Asia? *Stratigraphy and Geological Correlation*, 2, 130–150.
- Cisterna, A. G., & Shi, G. R. (2014). Lower Permian brachiopods from Wasp Head Formation, Sydney Basin, southeastern Australia. *Journal of Paleontology*, 88, 531–544.
- Clark, P. U., & Hansel, A. K. (1989). Clast ploughing, lodgement and glacier sliding over a soft glacier bed. *Boreas*, 18, 201–207.
- Collins, W. J. (2002a). Nature of extensional accretionary orogens. *Tectonics*, 21, 6–1 to 6–12.
- Collins, W. J. (2002b). Hot orogens, tectonic switching and creation of continental crust. *Geology*, 30, 535–538.
- Collins, W. J., & Hobbs, B. E. (2001). What caused the Early Silurian change from mafic to silicic (S-type) magmatism in the eastern Lachlan Fold Belt? *Australian Journal of Earth Sciences*, 48, 25–41.
- Collinson, J. D. (1996). Alluvial sediments. In H. D. Reading (Ed.), *Sedimentary environments: Processes, facies and stratigraphy*. Blackwell Publishing, 704.
- Collinson, J. D., & Thompson, D. B. (1989). *Sedimentary structures* (2nd ed.). London: Unwin Hyman. 207.
- Coney, P. J., Edwards, A., Hine, R., Morrison, F., & Windrum, D. (1990). The regional tectonics of the Tasman Orogenic system, eastern Australia. *Journal of Structural Geology*, 125, 19–43.
- Csato, I., & Catuneanu, O. (2012). Systems tract architecture under variable climatic and tectonic regimes: A quantitative approach. *Stratigraphy*, 9, 109–130.
- Csato, I., & Catuneanu, O. (2014). Quantitative conditions for the development of systems tracts. *Stratigraphy*, 11, 39–59.
- Csato, I., Catuneanu, O., & Granjeon, D. (2014). Millennial-scale sequence stratigraphy: Numerical simulation with Dionisos. *Journal of Sedimentary Research*, 84, 394–406.
- Dalrymple, R. W., & Choi, K. (2007). Morphologic and facies trends through the fluvial–marine transition in tide-dominated depositional systems: A schematic framework for environmental and sequence-stratigraphic interpretation. *Earth Science Reviews*, 81, 135–174.
- Dalrymple, R. W., Zaitlin, B. A., & Boyd, R. (1992). Estuarine facies models: conceptual basis and stratigraphic implications. *Journal of Sedimentary Petrology*, 62, 1130–1146.
- Dashtgard, S. E., Frey, S. E., & MacEachern, J. A. (2012). Tidal effects on the shoreface: Towards a conceptual framework. In S. G. Longhitano, D. Mellere, & R. B. Ainsworth (Eds.), *Modern and ancient depositional systems: Perspectives, models and signatures* (Vol. 279) (pp. 42–61). *Sedimentary Geology*.

- Dashtgard, S. E., & Gingras, M. K. (2007). Tidal controls on the morphology and sedimentology of gravel-dominated deltas and beaches: Examples from the megatidal Bay of Fundy, Canada. *Journal of Sedimentary Research*, 77, 1063–1077.
- Dashtgard, S. E., Gingras, M. K., & Butler, K. E. (2006). Sedimentology and stratigraphy of a transgressive, muddy gravel beach: Waterside Beach, Bay of Fundy, Canada. *Sedimentology*, 53, 279–296.
- Dashtgard, S. E., Gingras, M. K., & MacEachern, J. A. (2009). Tidally modulated shorefaces. *Journal of Sedimentary Research*, 79, 793–807.
- De Gasperi, A., & Catuneanu, O. (2014). Sequence stratigraphy of the Eocene turbidite reservoirs in the Albacora field, Campos Basin, offshore Brazil. *American Association of Petroleum Geologists Bulletin*, 98, 279–313.
- Di Celma, C., & Cantalamessa, G. (2007). Sedimentology and high-frequency sequence stratigraphy of a forearc extensional basin: The Miocene Caleta Herradura Formation, Mejillones Peninsula, northern Chile. *Sedimentary Geology*, 198, 29–52.
- Di Celma, C., Cantalamessa, G., Landini, W., & Ragaini, L. (2010). Stratigraphic evolution from shoreface to shelf-indenting channel depositional systems during transgression: Insights from the lower Pliocene Súa Member of the basal Upper Onzole Formation, Borbón Basin, northwest Ecuador. *Sedimentary Geology*, 223, 162–179.
- Di Celma, C., Ragaini, L., Cantalamessa, G., & Landini, W. (2005). Basin physiography and tectonic influence on the sequence architecture and stacking pattern: Pleistocene succession of the Canoa Basin (central Ecuador). *Geological Society of America Bulletin*, 117, 1226–1241.
- Dominguez, J. M. L., & Wanless, H. R. (1991). Facies architecture of a falling sea-level strandplain, Doce River coast, Brazil. In D. J. P. Swift, G. F. Oertel, W. Tillman, & J. A. Thorne (Eds.), *Shelf sand and sandstone bodies: Geometry, facies and sequence stratigraphy* (Vol. 14) (pp. 259–281). International Association of Sedimentologists Special Publication.
- Dumas, S., & Arnott, R. W. C. (2006). Origin of hummocky and swaley cross-stratification—The controlling influence of unidirectional current strength and aggradation. *Geology*, 34, 1073–1076.
- Dumas, S., Arnott, R. W. C., & Southard, J. B. (2005). Experiments on oscillatory-flow and combined-flow bed forms: Implications for interpreting parts of the shallow marine rock record. *Journal of Sedimentary Research*, 75, 501–513.
- Einsele, G., Ricken, W., & Seilacher, A. (1991). *Cycles and events in stratigraphy*. Berlin: Springer-Verlag. 955.
- Eriksson, P. G., Mazumder, R., Catuneanu, O., Bumby, A. J., & Ilordo, B. O. (2006). Precambrian continental freeboard and geological evolution: A time perspective. *Earth-Science Reviews*, 79, 165–204.
- Ethridge, F. G., Germanoski, D., Schumm, S. A., & Wood, L. J. (2001). The morphologic and stratigraphic effects of base-level change: A review of experimental studies. Seventh International Conference on Fluvial Sedimentology, Lincoln, August 6–10, Program and Abstracts, p. 95.
- Evans, P.R., Migliucci, A. (1991). Evolution of the Sydney Basin during the Permian as a foreland basin to the Curarong and New England orogens. Advances in the Study of the Sydney Basin, abstracts of the 25th Newcastle Symposium, pp. 22–27.
- Evans, D. J. A., Phillips, E. R., Hiemstra, J. F., & Auton, C. A. (2006). Subglacial till: Formation, sedimentary characteristics and classification. *Earth-Science Reviews*, 78, 115–176.
- Eyles, C. H., Eyles, N., & Gostin, V. A. (1998). Facies and allostratigraphy of high-latitude, glacially influenced marine strata of the Early Permian southern Sydney Basin, Australia. *Sedimentology*, 45, 121–161.
- Fanti, F., & Catuneanu, O. (2010). Fluvial sequence stratigraphy: The Wapiti Formation, west-central Alberta, Canada. *Journal of Sedimentary Research*, 80, 320–338.
- Feldman, H. R., Franseen, E. K., Joeckel, R. M., & Heckel, P. H. (2005). Impact of longer term modest climate shifts on architecture of high-frequency sequences (Cycloths), Pennsylvanian of Midcontinent U.S.A. *Journal of Sedimentary Research*, 75, 350–368.
- Fielding, C. R., Bann, K. L., MacEachern, J. A., Tye, S. C., & Jones, B. G. (2006). Cyclicity in the nearshore marine to coastal, Lower Permian, Pebbley Beach Formation, southern Sydney Basin, Australia: A record of relative sea-level fluctuations at the close of the Late Palaeozoic Gondwanan ice age. *Sedimentology*, 53, 435–463.
- Fielding, C. R., Frank, T. D., Birgenheier, L. P., Rygel, M. C., Jones, A. T., & Roberts, J. (2008). Stratigraphic imprint of the Late Palaeozoic Ice Age in eastern Australia: A record of alternating glacial and nonglacial climate regime. *Journal of the Geological Society*, 165, 129–140.
- Foster, D. A., Gray, D. R., & Bucher, M. (1999). Chronology of deformation within the turbidite dominated Lachlan orogen: Implications for the tectonic evolution of eastern Australia and Gondwana. *Tectonics*, 18, 452–485.
- Frey, S. E., & Dashtgard, S. E. (2012). Sedimentology, ichnology, and hydrodynamics of strait-margin, sand-and-gravel beaches and shorefaces: Juan de Fuca Strait, British Columbia, Canada. *Sedimentology*, 58, 1326–1346.
- Friedrichs, C. T., & Wright, L. D. (2004). Gravity-driven sediment transport on the continental shelf: Implications for equilibrium profiles near river mouths. *Coastal Engineering*, 51, 795–811.
- Gingras, M. K., Maceachern, J. A., & Dashtgard, S. E. (2011). Process ichnology and the elucidation of physico-chemical stress. *Sedimentary Geology*, 237, 115–134.
- Gingras, M. K., Maceachern, J. A., Dashtgard, S. H., Zonneveld, J.-P., Schoengut, J., Ranger, M. J., & Pemberton, S. G. (2012). Estuaries. *Developments in Sedimentology*, 64, 463–505.
- Gingras, M. K., Pemberton, S. G., & Saunders, T. (2000). Firmness profiles associated with tidal-creek deposits: The temporal significance of *Glossifungites* assemblages. *Journal of Sedimentary Research*, 70, 1017–1025.
- Glen, R. A. (2013). Refining accretionary orogen models for the Tasmanides of eastern Australia. *Australian Journal of Earth Sciences*, 60, 315–370.
- Glen, R. A., & Beckett, J. (1997). Structure and tectonics along the inner edge of a foreland basin: The Hunter Coalfield in the northern Sydney Basin, New South Wales. *Australian Journal of Earth Sciences*, 44, 853–877.
- Golledge, N. R. (2007). Sedimentology, stratigraphy, and glacier dynamics, western Scottish Highlands. *Quaternary Research*, 68, 79–95.
- Gostin, V. A., & Herbert, C. (1973). Stratigraphy of the Upper Carboniferous and Lower Permian sequence, southern Sydney Basin. *Journal of the Geological Society of Australia*, 20, 49–70.
- Gray, D. R., Foster, D. A., & Bierlein, F. (2002). Geodynamics and metallogeny of the Lachlan Orogen. *Australian Journal of Earth Sciences*, 49, 1041–1056.
- Hampson, G. J. (2010). Sediment dispersal and quantitative stratigraphic architecture across an ancient shelf. *Sedimentology*, 57, 96–141.
- Hampson, G. J., & Storms, J. E. A. (2003). Geomorphological and sequence stratigraphic variability in wave-dominated, shoreface-shelf parasequences. *Sedimentology*, 50, 667–701.
- Holland-Hansen, W., & Martinsen, O. J. (1996). Shoreline trajectories and sequences: Description of variable depositional-dip scenarios. *Journal of Sedimentary Research*, 66, 670–688.
- Herbert, C., Helby, R. (1980). A guide to the Sydney Basin. Geological Survey NSW Bulletin 26, 603 pp.
- Isbell, J. L., Cole, D. I., & Catuneanu, O. (2008). Carboniferous-Permian glaciation in the main Karoo Basin, South Africa: Stratigraphy, depositional controls, and glacial dynamics. In C. R. Fielding, T. D. Frank, & J. L. Isbell (Eds.), *Resolving the Late Paleozoic ice age in time and space* (Vol. 441) (pp. 71–82). Geological Society of America Special Paper.
- Isbell, J. L., Miller, M. F., Wolfe, K. L., & Lenaker, P. A. (2003). Timing of late Paleozoic glaciations in Gondwana: Was glaciation responsible for the development of Northern Hemisphere cyclothems? *Geological Society of America Special Papers*, 370, 5–24.
- Joeckel, R. M., & Korus, J. T. (2012). Bayhead delta interpretation of an Upper Pennsylvanian sheetlike sandbody and the broader

- understanding of transgressive deposits in cyclothems. *Sedimentary Geology*, 275–276, 22–37.
- Jones, A. T., & Fielding, C. R. (2004). Sedimentological record of the late Palaeozoic glaciation in Queensland, Australia. *Geology*, 32, 153–156.
- Keen, T. R., Furukawa, Y., Bentley, S. J., Slingerland, R. L., Teague, W. J., Dykes, J. D., & Rowley, C. D. (2006). Geological and oceanographic perspectives on event bed formation during Hurricane Katrina. *Geophysical Research Letters*, 33, L23614. <https://doi.org/10.1029/2006GL027981>
- Kidwell, S. M. (1991). Condensed deposits in siliciclastic sequences: Expected and observed features. In G. Einsele, W. Ricken, & A. Seilacher (Eds.), *Cycles and events in stratigraphy* (pp. 682–695). Berlin: Springer-Verlag.
- Kidwell, S. M. (1997). Anatomy of extremely thin marine sequences landward of a passive-margin hinge zone: Neogene Calvert Cliffs succession, Maryland, U.S.A. *Journal of Sedimentary Research*, 67, 322–340.
- Leckie, D. A., & Walker, R. G. (1982). Storm and tide dominated shorelines in Late Cretaceous Moosebar-lower Gates interval—Outcrop equivalents of Deep Basin gas traps in Western Canada. *American Association of Petroleum Geologists Bulletin*, 66, 138–157.
- Legler, B., Johnson, H. D., Hampson, G. J., Massart, B. Y. G., Jackson, C. A. L., Jackson, M. D., ... Ravnas, R. (2013). Facies model of a fine-grained, tide-dominated delta: Lower Dir Abu Lifa Member (Eocene), Western Desert, Egypt. *Sedimentology*, 60, 1313–1356.
- Levoy, F., Monfort, O., & Larsson, C. (2001). Hydrodynamic variability on megatidal beaches, Normandy, France. *Continental Shelf Research*, 21, 563–586.
- Løseth, T. M., Steel, R. J., Crabaugh, J. P., & Schellpeper, M. (2006). Interplay between shoreline migration paths, architecture and pinchout distance for siliciclastic shoreline tongues: Evidence from the rock record. *Sedimentology*, 53, 735–767.
- Lowe, D. R. (1976). Subaqueous liquified and fluidized sediment flows and their deposits. *Sedimentology*, 23, 285–308.
- Lowe, D. R. (1988). Suspended-load fallout rate as an independent variable in the analysis of current structures. *Sedimentology*, 35, 765–776.
- MacEachern, J. A., & Bann, K. L. (2008). The role of ichnology in refining shallow marine facies models. In G. J. Hampson, R. J. Steel, P. M. Burgess, & R. W. Dalrymple (Eds.), *Recent advances in models of siliciclastic shallow-marine stratigraphy* (Vol. 90) (pp. 73–116). SEPM Special Publications.
- MacEachern, J. A., Raychaudhuri, I., & Pemberton, S. G. (1992). Stratigraphic applications of the *Glossifungites* ichnofacies: Delineating discontinuities in the rock record. In S. G. Pemberton (Ed.), *Applications of ichnology to petroleum exploration* (Vol. 17) (pp. 169–198). SEPM Core Workshop.
- Mackay, D. A., & Dalrymple, R. W. (2005). A sedimentological comparison of tide-dominated estuarine and tide-dominated deltaic deposits: A subsurface perspective. Abstracts: Annual Meeting-American Association of Petroleum Geologists, p. A84
- Magalhães, A. J. C., Scherer, C. M. S., Raja Gabaglia, G. P., Ballico, M. B., & Catuneanu, O. (2014). Unincised fluvial and tide-dominated estuarine systems from the Mesoproterozoic lower Tombador formation, Chapada Diamantina basin, Brazil. *Journal of South American Earth Sciences*, 56, 68–90.
- Magalhães, A. J. C., Scherer, C. M. S., Raja Gabaglia, G. P., & Catuneanu, O. (2015). Mesoproterozoic delta systems of the Açuá Formation, Chapada Diamantina, Brazil. *Precambrian Research*, 257, 1–21.
- Maravelis, A. G., Boutelier, D., Catuneanu, O., Seymour, K. S., & Zelilidis, A. (2016). A review of tectonics and sedimentation in a forearc setting: Hellenic Thrace Basin, north Aegean Sea and mainland Greece. *Tectonophysics*, 674, 1–19.
- Maravelis, A., Konstantopoulos, P., Pantopoulos, G., & Zelilidis, A. (2007). North Aegean sedimentary basin evolution during the Late Eocene to Early Oligocene based on sedimentological studies on Lemnos Island (NE Greece). *Geologica Carpathica*, 58, 455–464.
- Maravelis, A., Makrodimitis, G., Pasadakis, N., & Zelilidis, A. (2014). Stratigraphic evolution and source rock potential of a Lower Oligocene–Lower/Middle Miocene continental slope system, Greek Fold and Thrust Belt, Ionian Sea, Northwest Greece. *Geological Magazine*, 151(3), 394–413.
- Maravelis, A. G., Pantopoulos, G., Tserolas, P., & Zelilidis, A. (2017). Reply to comment by Caracciolo, L., Meinhold, G., Critelli, S., von Eynatten, H., & Manetti, P., on: Maravelis, A. G., Pantopoulos, G., Tserolas, P., & Zelilidis, A., 2015. "Accretionary prism forearc interactions as reflected in the sedimentary fill of southern Thrace Basin (Lemnos Island, NE Greece)". *International Journal of Earth Sciences*, 106, 389–394.
- Maravelis, A., & Zelilidis, A. (2011). Geometry and sequence stratigraphy of the Late Eocene–Early Oligocene shelf and basin floor to slope turbidite systems, Lemnos Island, NE Greece. *Stratigraphy and Geological Correlation*, 19, 205–220.
- Maravelis, A. G., & Zelilidis, A. (2012). Paleoclimatology and paleoecology across the Eocene/Oligocene boundary, Thrace Basin, Northeast Aegean Sea, Greece. *Palaeogeography, Palaeoclimatology, Palaeoecology*, 365–366, 81–98.
- Martins-Neto, M., & Catuneanu, O. (2010). Rift sequence stratigraphy. *Journal of Marine and Petroleum Geology*, 27, 247–253.
- McCabe, P. (1977). Deep distributary channels and giant bedforms in the Upper Carboniferous of the Central Pennines, northern England. *Sedimentology*, 24, 271–290.
- Medici, G., Boulesteix, K., Mountney, N. P., West, L. J., & Odling, N. E. (2015). Palaeoenvironment of braided fluvial systems in different tectonic realms of the Triassic Sherwood Sandstone Group, UK. *Sedimentary Geology*, 329, 188–210.
- Miall, D. (1977). A review of the braided-river depositional model environment. *Earth-Science Reviews*, 13, 1–62.
- Miall, A. D., Catuneanu, O., Vakarelov, B. K., & Post, R. (2008). The Western interior basin. In A. D. Miall, & K. J. Hsu (Eds.), *The sedimentary basins of the United States and Canada. Sedimentary basins of the world* (pp. 329–362). Amsterdam: Elsevier.
- Milana, J. P., & Tietze, K. W. (2007). Limitations of sequence stratigraphic correlation between marine and continental deposits: A 3D experimental study of unconformity-bounded units. *Sedimentology*, 54, 293–316.
- Monegato, G., & Stefani, C. (2010). Stratigraphy and evolution of a long-lived fluvial system in the southeastern Alps (NE Italy): The Tagliamento conglomerate. *Austrian Journal of Earth Sciences*, 103, 33–49.
- Naish, T. R., & Wilson, G. S. (2009). Constraints on the amplitude of mid-Pliocene (3.6–2.4 Ma) eustatic sea-level fluctuations from the New Zealand shallow-marine sediment record. *Philosophical Transactions of the Royal Society*, 367, 169–187.
- Nemec, W., & Postma, G. (1993). Quaternary alluvial fans in southwestern Crete: Sedimentation processes and geomorphic evolution. In M. Marzo, & C. Puigdefabregas (Eds.), *Alluvial sedimentation*. Oxford, UK: Blackwell Publishing Ltd. <https://doi.org/10.1002/9781444303995.ch18>
- Nemec, W., & Steel, R. (1984). Alluvial and coastal conglomerates: Their significant features and some comments on gravelly mass-flow deposits. *Sedimentology of gravels and conglomerates*. Canadian Society of Petroleum Geologists Memoir, 10, 1–31.
- Nichols, G. (2009). *Sedimentology and stratigraphy*. Wiley-Blackwell. 432.
- Nichols, G., & Fisher, J. A. (2007). Processes, facies and architecture of fluvial distributary system deposits. *Sedimentary Geology*, 195, 75–90.
- Offler, R., McKnight, S., & Morand, V. (1998). Tectonothermal history of the western Lachlan Fold Belt, Australia: Insights from white mica studies. *Journal of Metamorphic Geology*, 16, 531–540.
- Offler, R., Miller, J., Grayd, R., Foster, D. A., & Bale, R. (1998). Crystallinity and  $b_0$  spacing of K-white micas in a Paleozoic accretionary complex, eastern Australia: Metamorphism, paleogeotherms, and structural style of an underplated sequence. *Journal of Geology*, 106, 495–509.
- Olariu, M. I., Olariu, C., Steel, R. J., Dalrymple, R. W., & Martinus, A. W. (2012). Anatomy of a laterally migrating tidal bar in front of a delta

- system: Esdolomada Member, Roda Formation, Tremp-Graus Basin, Spain. *Sedimentology*, 59, 356–378.
- Pattison, S. A. J., Ainsworth, R. B., & Hoffman, T. A. (2007). Evidence of across-shelf transport of fine-grained sediments: Turbidite-filled shelf channels in the Campanian Aberdeen Member, Book Cliffs, Utah, USA. *Sedimentology*, 54, 1033–1064.
- Pemberton, G. S., Spila, M., Pulham, A. J., Saunders, T., MacEarhern, J. A., Robbins, D., & Sinclair, I. K. (2002). Ichnology and sedimentology of shallow marine to marginal marine systems: Ben Nevis and Avalon Reservoirs, Jeanne d'Arc Basin. *Geological Association of Canada, Short Course Notes*, 15, 343 pp.
- Peters, S. E., & Loss, D. P. (2012). Storm and fair-weather wave base: A relevant distinction? *Geology*, 40(6), 511–514.
- Piotrowski, J. A. (1994). Waterlain and lodgement till facies of the lower sedimentary complex from the Danischer Wohld cliff, Schleswig-Holstein, North Germany. In W. P. Warren, & D. G. Croot (Eds.), *Formation and deformation of glacial deposits* (pp. 3–8). Rotterdam: Balkema.
- Plint, A. G., & Nummedal, D. (2000). The falling stage systems tract: Recognition and importance in sequence stratigraphic analysis. In D. Hunt, & R. L. Gawthorpe (Eds.), *Sedimentary responses to forced regressions* (Vol. 172) (pp. 1–17). Geological Society Special Publication.
- Plint, A. G., & Wadsworth, J. A. (2003). Sedimentology and palaeogeomorphology of four large valley systems incising delta plains, western Canada Foreland Basin: Implications for mid-Cretaceous sea-level changes. *Sedimentology*, 50, 1147–1186.
- Pontén, A., & Plink-Björklund, P. (2007). Depositional environments in an extensive tide-influenced delta plain, Middle Devonian Gauja Formation, Devonian Baltic Basin. *Sedimentology*, 54, 969–1006.
- Posamentier, H. W., & Allen, G. P. (1999). Siliciclastic sequence stratigraphy –Concepts and applications. *SEPM Concepts in Sedimentology and Paleontology*, 7, 210.
- Reading, H. G., & Collinson, J. D. (1996). Clastic coasts. In H. G. Reading (Ed.), *Sedimentary environments: Processes, facies and stratigraphy* (pp. 154–231). Oxford: Blackwell Science.
- Reineck, H. E., & Wunderlich, F. (1968). Classification and origin of flaser and lenticular bedding. *Sedimentology*, 11, 99–104.
- Retallack, G. J. (1999). Permafrost palaeoclimate of Permian palaeosols in the Gerringong volcanic facies of New South Wales. *Australian Journal of Earth Sciences*, 46, 11–22.
- Reynaud, J. Y., Ferrandini, M., Ferrandini, J., Sandigo, M., Thimon, I., Andre, J. P., ... Tessier, B. (2013). From non-tidal shelf to tide-dominated strait: The Miocene Bonifacio Basin, Southern Corsica. *Sedimentology*, 60, 599–623.
- Rossi, V., & Steel, R. J. (2016). The role of tidal, wave and river currents in the evolution of mixed-energy deltas: Example from the Lajas Formation (Argentina). *Sedimentology*, 63, 824–864.
- Rygel, M. C., Fielding, C. R., Bann, K. L., Frank, T. D., Birgenheier, L., & Tye, S. C. (2008a). The Lower Permian Wasp Head Formation, Sydney Basin: High-latitude, shallow marine sedimentation following the late Asselian to early Sakmarian glacial event in eastern Australia. *Sedimentology*, 55, 1517–1540.
- Rygel, M. C., Fielding, C. R., Frank, T. D., & Birgenheier, L. P. (2008b). The magnitude of Late Paleozoic glacioeustatic fluctuations: A synthesis. *Journal of Sedimentary Research*, 78, 500–511.
- Sageman, B. B. (1996). Lowstand tempestites: Depositional model for cretaceous skeletal limestones, western interior basin. *Geology*, 24, 888–892.
- Scheibner, E. (1987). Paleozoic tectonic development of eastern Australia in relation to the Pacific region. In E. C. Leitch, & E. Scheibner (Eds.), *Terrane accretion and orogenic belts* (Vol. 19) (pp. 133–165). American Geophysical Union Geodynamic.
- Scheibner, E., & Vevers, J. J. (2000). Tasman fold belt system. In J. J. Vevers (Ed.), *Billion-year earth history of Australia & neighbours in Gondwanaland* (pp. 164–234). Sydney: GEMOC Press.
- Scott, E. S. (1992). The palaeoenvironments and dynamics of the Rannoch-Etive nearshore and coastal succession, Brent Group, northern North Sea. In A. C. Morton, R. S. Haszledine, M. R. Giles, & S. R. Brown (Eds.), *Geology of the Brent Group* (Vol. 61) (pp. 129–148). Geological Society of London Special Publication.
- Selleck, B. W., Carr, P. F., & Jones, B. G. (2007). A review and synthesis of glendonites (pseudomorphs after ikaite) with new data: Assessing applicability as recorders of ancient coldwater conditions. *Journal of Sedimentary Research*, 77, 908–991.
- Sloss, L. L., Krumbein, W. C., & Dapples, E. C. (1949). Integrated facies analysis. In C. R. Longwell (Ed.), *Sedimentary facies in geologic history* (Vol. 39) (pp. 91–124). Geological Society of America Memoirs.
- Spaggiari, C. V., Gray, D. R., & Foster, D. A. (2003). Tethyan- and Cordilleran-type ophiolites of eastern Australia: Implications for the evolution of the Tasmanides. In Y. Dilek, & P. T. Robinson (Eds.), *Ophiolites in Earth history* (Vol. 218) (pp. 517–539). Special Publication of the Geological Society London.
- Stear, W. M. (1978). Sedimentary structures related to fluctuating hydrodynamic conditions in flood plain deposits of the Beaufort Group near Beaufort West, Cape. *Transactions of the Geological Society of South Africa*, 81, 393–399.
- Steel, R. J., & Thompson, D. B. (1983). Structures and textures in the Triassic braided stream conglomerates ('Bunter' Pebble Beds) in the Sherwood Sandstone Group, North Staffordshire, England. *Sedimentology*, 30, 341–367.
- Swenson, J. B., & Muto, T. (2007). Response of coastal plain rivers to falling relative sea-level: Allogenic controls on the aggradational phase. *Sedimentology*, 54, 207–221.
- Thomas, S. G., Fielding, C. R., & Frank, T. D. (2007). Lithostratigraphy of the late Early Permian (Kungurian) Wandrawandian Siltstone, New South Wales: Record of glaciation? *Australian Journal of Earth Sciences*, 54, 1057–1071.
- Tye, S. C., Fielding, C. R., & Jones, B. G. (1996). Stratigraphy and sedimentology of the Permian Talaterang and Shoalhaven Groups in the southernmost Sydney Basin, New South Wales. *Australian Journal of Earth Sciences*, 43, 57–69.
- Vevers, J. J., Belousova, E. A., Saeed, A., Sircombe, K., Cooper, A. F., & Read, S. E. (2006). Pan-Gondwanaland detrital zircons from Australia analysed for Hf-isotopes and trace elements reflect an ice-covered Antarctic provenance of 700–500 Ma age,  $T_{DM}$  of 2.0–1.0 Ga, and alkaline affinity. *Earth-Science Reviews*, 76, 135–174.
- Vevers, J. J., Conaghan, P. J., & Powell, C. M. (1994). Eastern Australia, Permian-Triassic Pangean Basins and Foldbelts along the Panthalassan Margin of Gondwanaland. Boulder, CO, USA. *Geological Society of America*, 174, 11–171.
- Vermeij, G. J., & Dudley, E. C. (1985). Distribution of adaptation: A comparison between the functional shell morphology of freshwater and marine pelecypods. *The Mollusca*, 10, 461–478.
- Visser, M. J. (1980). Neap-spring cycles reflected in Holocene subtidal large-scale bedform deposits: A preliminary note. *Geology*, 8, 543–546.
- Walker, R. G., & Plint, A. G. (1992). Wave and storm dominated shallow marine systems. In R. G. Walker, & N. P. James (Eds.), *Facies models: Responses to sea level change* (pp. 219–238). Geological Association of Canada.
- Whiting, P. J., Dietrich, W. E., Leopold, L. B., Drake, T. G., & Shreve, R. L. (1988). Bedload sheets in heterogeneous sediment. *Geology*, 16, 105–108.
- Yokokawa, M., Masuda, F., & Endo, N. (1995). Sand particle movement on migrating combined-flow ripples. *Journal of Sedimentary Research*, 65, 40–44.
- Zecchin, M. (2005). Relationships between fault-controlled subsidence and preservation of shallow-marine small-scale cycles: Example from the lower Pliocene of the Crotone Basin (southern Italy). *Journal of Sedimentary Research*, 75, 300–312.

- Zecchin, M. (2007). The architectural variability of small-scale cycles in shelf and ramp clastic systems: The controlling factors. *Earth-Science Reviews*, 84, 21–55.
- Zecchin, M., Caffau, M., Civile, D., & Roda, C. (2010). Anatomy of a late Pleistocene clinoformal sedimentary body (Le Castella, Calabria, southern Italy): A case of prograding spit system? *Sedimentary Geology*, 223, 291–309.
- Zecchin, M., & Catuneanu, O. (2013). High-resolution sequence stratigraphy of clastic shelves I: Units and bounding surfaces. *Marine and Petroleum Geology*, 39, 1–25.
- Zecchin, M., & Catuneanu, O. (2015). High-resolution sequence stratigraphy of clastic shelves III: Applications to reservoir geology. *Marine and Petroleum Geology*, 62, 161–175.
- Zecchin, M., Catuneanu, O., & Rebesco, M. (2015). High-resolution sequence stratigraphy of clastic shelves IV: High-latitude settings. *Marine and Petroleum Geology*, 68, 427–437.
- Zecchin, M., Civile, D., Caffau, M., Sturiale, G., & Roda, C. (2011). Sequence stratigraphy in the context of rapid regional uplift and high-amplitude glacio-eustatic changes: The Pleistocene Cutro Terrace (Calabria, southern Italy). *Sedimentology*, 58, 442–477.

**How to cite this article:** Maravelis AG, Catuneanu O, Nordsvan A, Landenberger B, Zelilidis A. Interplay of tectonism and eustasy during the Early Permian icehouse: Southern Sydney Basin, southeast Australia. *Geological Journal*. 2018;53:1372–1403. <https://doi.org/10.1002/gj.2962>